

Simulation of Drift Chamber Performance in Magnetic Fields

Mikhail V. Kossov, Mac Mestayer

Continuous Electron Beam Accelerator Facility

Newport News, VA 23606

April 23, 1993

ABSTRACT

The arrival time for the electrons has been simulated for different tracks passing through the hexagonal drift chamber cell with the magnetic field directed along the wire. The resulting arrival time is parametrized as a function of the distance of closest approach, the track incident angle to the axis of the hexagonal cell projected onto the midplane (0-30 degrees), and the magnetic field (0., 0.5, 1., and 1.5 Tesla). The simulations have been done for cells with radius 1.4 cm and HV=2.5 kV. The parametrizations can be used for the simulation and reconstruction of the tracks in the CLAS detector.

Introduction

The effect of magnetic field on drift velocity was measured and discussed for a wire drift chamber with an hexagonal cell geometry and an argon-ethane (50:50) gas mixture [1]. In this work the new version 3.0 of the simulation program GARFIELD [2] has been used for the simulation of the arrival time (t) depending on the distance of the closest approach of the straight track to the wire (x), the incident tracks angle to the axis of the hexagon cell (Θ_{tr}), and the magnetic field (B) directed along the wire. The simulated correlation distribution has been parametrized for practical applications.

To describe $t(x)$ dependence a four parameter polynomial function was used. The parameters are functions of B and Θ_{tr} . The polynomial approximation can not be reversed, that is there does not exist an algebraic function for the $x(t)$ dependence. To use the Newton method for the $x(t)$ simulation the first guess for x is needed. For this purpose the $t(x)$ was parametrized roughly as $t = x * (a + b * x)$. Both parameters depend on Θ_{tr} and B . This parametrization can be easily reversed and can be used for a fast simulation and fast reconstruction.

The simulation revealed the significance of the long-time signals which corresponds to the large distances of closest approach. Experimentally the time range was investigated only for the hexagonal cell with 1. cm radius [1]. The measured drift time was less then 500 ns for the distances less then 1. cm. In this region of x and t our simulated distribution for the 1.4 cm cell coincides with the measured one but in addition gives drift times longer then 1000 ns for distances up to 1.6 cm. So if the long distance efficiency at high magnetic field is important then the appropriate time gate should be used.

It was stated in [1] that for a magnetic field 1.5 Tesla the minimal drift time corresponds to the angle $\Theta_{tr} = -17^\circ$ and the maximal drift time corresponds to the angle $\Theta_{tr} = 13^\circ$ (like for $B = 0$ they are 30° and 0°). Our simulation shows that at present accuracy of our calculations the $x(t)$ plot can be parametrized as a function of $\cos(\alpha)$, where $\alpha = 6 \cdot (\Theta_{tr} + 10(\frac{\text{degrees}}{\text{Tesla}}) \cdot B(\text{Tesla}))$. (the factor 6 before Θ_{tr} reflects 6 fold symmetry of the cell). Thus for the magnetic field 1.5 Tesla we estimate the angle of minimal drift time to be -15° ($\cos(\alpha) = 1$) and the angle of maximal drift time to be 15° ($\cos(\alpha) = -1$). Both parameters are close to that obtained in [1].

GARFIELD simulation.

There are two possibilities in GARFIELD to simulate the drift time for the track: XT-PLOT package and ARRIVAL-TIME-DISTRIBUTION package. XT-PLOT searches for each point of track the shortest drift-line, disregarding clustering effects but informing about the diffusion to be expected on that shortest drift-line. In fact the $x(t)$ correlation is a result of the numerical solution of the equation of motion for the electrons.

The ARRIVAL package operates on the same track as XT-PLOT does, but in addition assumes the readout triggers at a given electron count. On each track the clusters are generated specified number of times, for each cluster the drift time is computed and the histogram of the arrival time for n electrons is filled. We used the arrival time for the first electron ($n=1$ is a default value), but it can be changed depending on the electronics requirements. The Monte-Carlo nature of the ARRIVAL computations makes the results less precise than those produced by XT-PLOT (because of the statistical error of the calculation) but what is computed is closer to what is actually measured because it takes into account the effect of the. For example, if a track comes through the wire then XT-PLOT obviously gives a zero value of the minimal drift-time, but because of the the measured drift-time will have nonzero value comparable with a half of the mean distance between clusters. This effect is simulated by ARRIVAL package. On the other hand, the statistical error can be made small in ARRIVAL by choosing proper binning and requesting a large number of iterations.

For the simulation we selected ARRIVAL package of GARFIELD. The price was a long time of calculation, but it was inevitable for the drift cell placed in the magnetic field, because at $B=1.5$ Tesla the XT-PLOT could not solve the equations of motion or could not find a minimum time. In both cases the information was marked as bad and could not be used for the approximation.

Table 1. The parameters of the drift cell ($R = 1.4cm$)

Parameter	Sense wire	Potential wire	Guard wire
Diameter of Wire (cm)	0.002	0.014	0.015
HV (kV)	+1700	-850	+600

The test grid of wires used for the simulation is shown in Fig.1. The cell in the middle of the grid was used for the simulation. To simulate the response of the drift chamber model only straight vertical tracks were used but the grid was rotated. We simulated Drift-time - Distance-closest-approach dependence for the 12 angles: $\Theta_{tr} = 0^\circ - 55^\circ$ (for $B = 0$ only 7 angles $\Theta_{tr} = 0^\circ - 55^\circ$). The parameters of the cell (HV and diameters of the wires) are shown in a Table 1. In Fig.2 the drift paths

are shown for $B=1$ Tesla. One can see that for the nonzero magnetic field the track can be detected even beyond the cell.

It should be noted that ARRIVAL simulation has one significant disadvantage. The positions of all clusters are defined only by starting point of the track and are not randomized. That is why for a fixed starting point of a track the shortest drift time always fixed and long drift times has fixed systematic errors which can not be avoided by increasing of statistics or a number of bins in histograms. The possibility of cluster position randomization should be used for final calculations.

A typical example of the XT-PLOT output ($B=0$) is shown in Fig.3. The only curve corresponds to the shortest drift time. An example of the ARRIVAL output ($B=1$ Tesla) is shown in Fig.4. There are three curves. The solid curve is the mean arrival time of all electrons from the track, the dashed line is the mean time for the arrival of the second electrons the dotted line is the time at which any electron have 0.5 chance to have arrived. There is another dotted line which practically coincides with the dashed one. This line corresponds to the time at which second electron have 0.5 chance to have arrived.

Approximation.

The correlation $t(x)$ distribution simulated by GARFIELD are shown in Fig.5(a-l) for different angles Θ_{tr} . In each figure one can see four distributions for four values of magnetic field. The curves corresponds to the approximation:

$$t(x) = x \cdot (p_1 + x^2 \cdot (p_2 + x^4 \cdot (p_3 + x^8 \cdot p_4))).$$

The p_i parameters have been found for each B and Θ_{tr} and then the p_i parameters have been parametrized as functions of B and Θ_{tr} . As a result of the approximation it was found that:

$$p_1 = 0.1846 + 0.01685 \cdot B^{1.861}$$

$$p_2 = 0.018 + 0.192 \cdot B^2 - 0.002 \cdot e^{2B} * \cos(6 \cdot (\Theta_{tr} - 10 \cdot B))$$

$$p_3 = -0.005 - 0.04627 \cdot B^{3/2}$$

$$p_4 = 0.001 + .0004 \cdot B + 0.0002 * (1. + \cos(6 \cdot (\Theta_{tr} + 10 \cdot B))).$$

The magnetic field is measured in Tesla and the angle in degrees, drift time in microseconds and distance of closest approach in centimeters. No special reasons

for this for was used. It was found the best of tested 4-parameter forms. The low x part is not shown because it depends on the starting condition (the clusters are not randomized in ARRIVAL and for the same starting conditions cluster distribution is the same, as a result the minimal arrival time for $x = 0$ is fixed for the same starting point of track). Trying different initial conditions the most probable minimal arrival time (t_{min}) was found to be equal to 1.5 ns, but the distribution of t_{min} has a long tail and the mean value equals 4.5 ns.

The curve of the fit is close enough to the simulated points but the polynomial is algebraic nonreversible. To find numerically $x(t)$ function one needs the guess for the first approximation. For this purpose simple $t(x)$ parametrization has been done. The result of the approximation by function $t(x) = x * (a + b * x)$, where

$$a = 0.1433 + .00444 \cdot (B - 0.5)^2 + 0.01 \cdot 2^{2B} \cdot \cos(6 \cdot (\Theta_{tr} + 10 \cdot B))$$

$$b = e^{-3.42+2.38 \cdot B-0.6 \cdot B^2} + (0.015 + 0.025 \cdot B + 0.03 \cdot B^2) \cdot \cos(6 \cdot \alpha + 60 \cdot B)$$

is shown in Fig.6(a-1). The approximation is rough but the function can be easy reversed and can be used not only as a first approximation for the numerical calculation of $x(t)$ function but as well for the fast simulation and recognition debugging of the Drift Chambers software.

Future development of the analysis.

The calculations are time capacitive, so before the calculations with large statistical accuracy could be done one should fix cell geometry, gas mixture, HV etc. The simulation should be done for the magnetic field stronger then 1.5 Tesla and for some angle between wire and and a magnetic field. To improve an accuracy of reconstruction it is significant to estimate the dependence of the resolution and to simulate the results of the real measurements [1]. At last, one could reduce the systematic errors of the approximation using the parametrization of $p_i(B, \Theta_{tr})$ functions not by the purely empirical function (like it was done in this paper) but by a function which bases on the physics of the drift process.

Figure captions.

Fig.1. The test grid of wires used for the simulation. The grid is rotated for some angle and the test track is always vertical.

Fig.2. The drift paths for $B=1$ Tesla.

Fig.3. An example of the XT-PLOT output ($B=0$) (GARFIELD).

Fig.4. An example of the ARRIVAL output ($B=1$ Tesla) (GARFIELD).

Fig.5. Parametrization of the $t(x)$ dependence by nonreversible polynomial function (see text). Different curves correspond to the different magnetic field and different pictures (a-1) to the different Θ_{tr} .

Fig.6. Parametrization of the $t(x)$ dependence by reversible polynomial dependence $t = x(a + bx)$ Different curves correspond to the different magnetic field and different pictures (a-1) to the different Θ_{tr} .

References

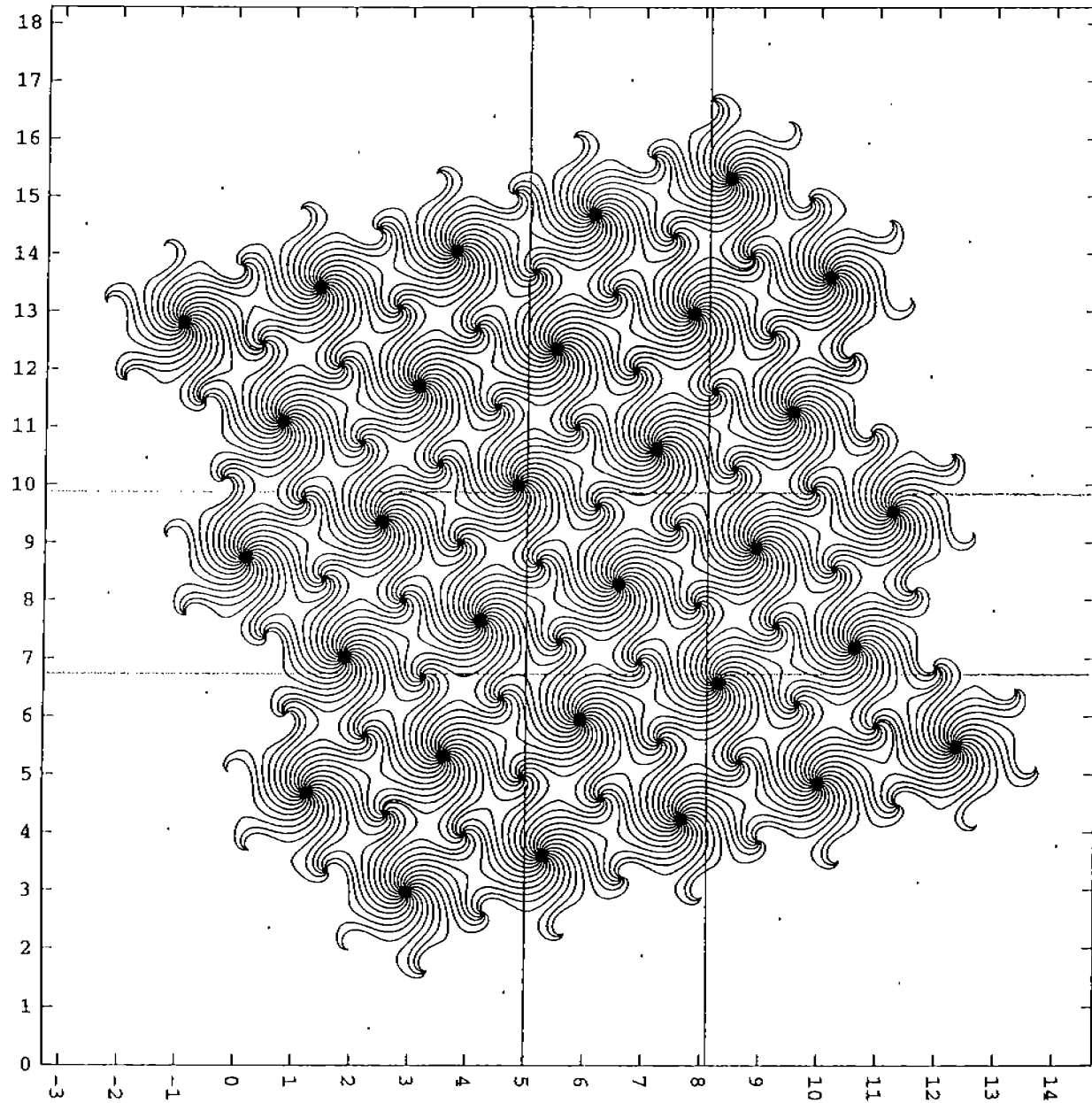
- 1) M.D.Mestayer et al., IEEE Transactions on Nuclear Science, **39** (1992) 690.
- 2) R.Veenhof, "Garfield, a drift-chamber simulation program, Version 3.00", CERN, 1991.

WIRE DRIFT LINE PLOT

Particle ID= Electron

Gas ID =Argon 50% Ethane 50%

y-axis [cm]



Plotted at 10:31:02 on 23/04/93 with Garfield version 4.06.

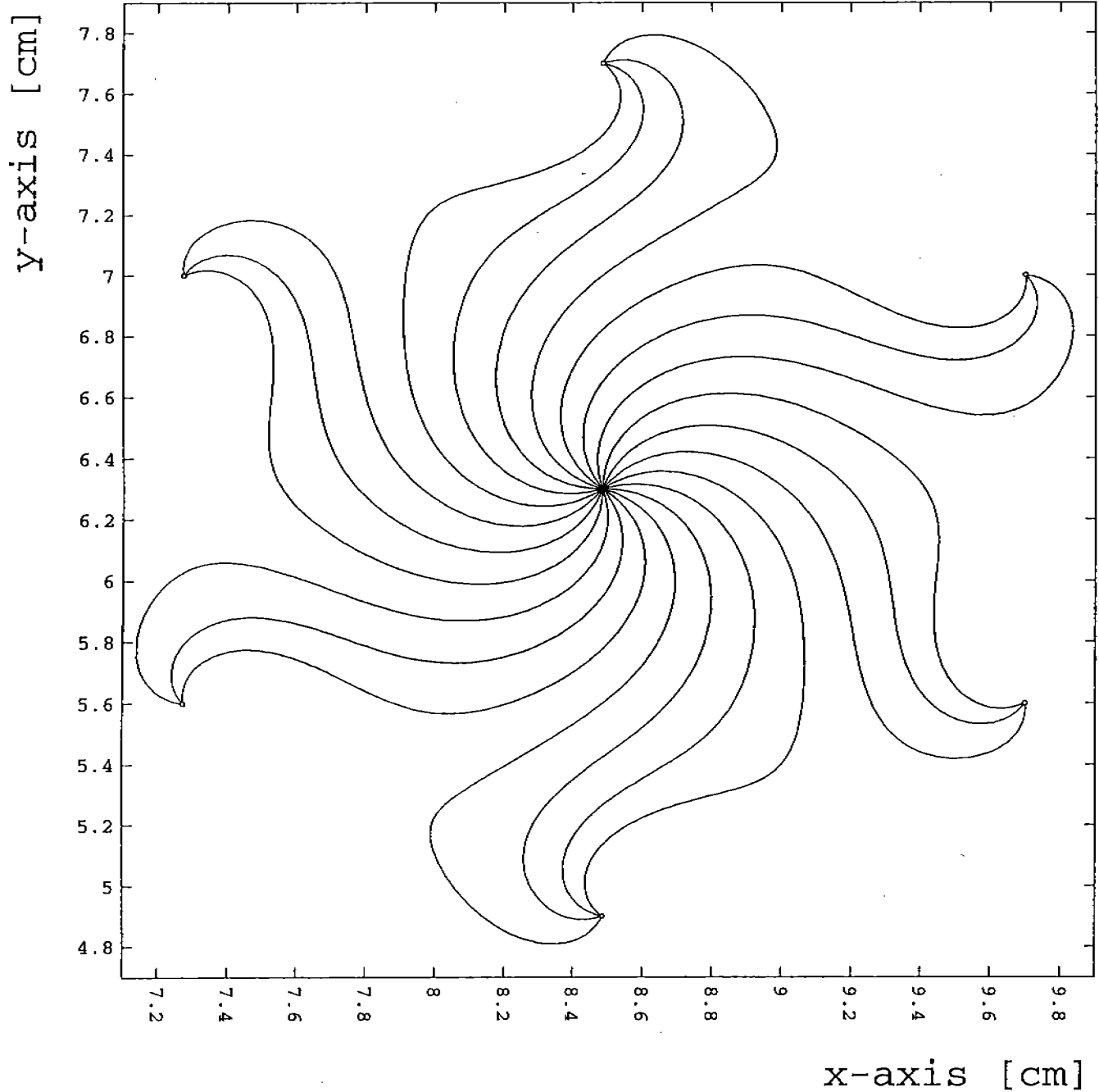
Fig.1 Drift chamber model

x-axis [cm]

WIRE DRIFT LINE PLOT

Particle ID= Electron

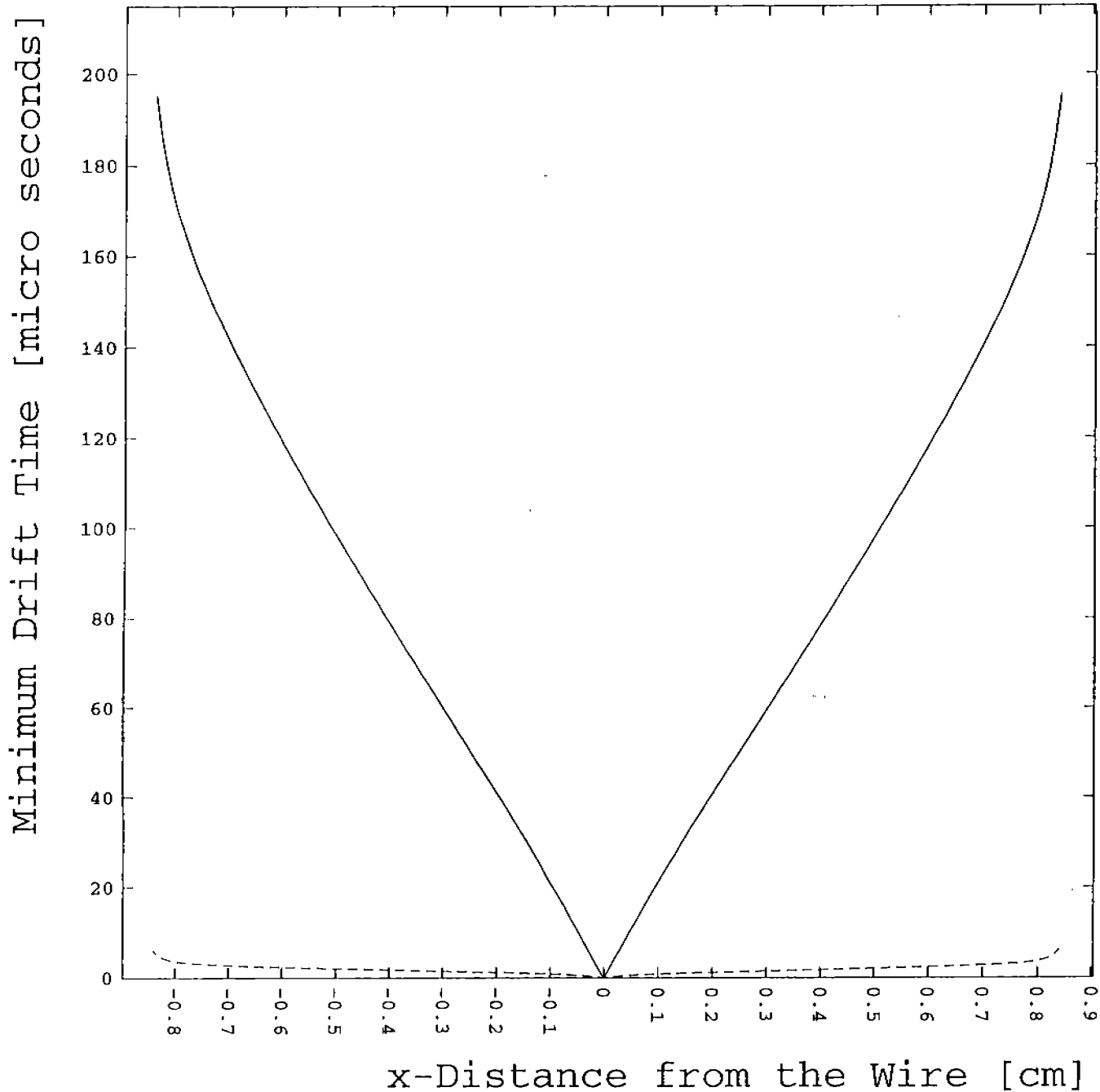
Gas ID =Argon 50% Ethane 50%



Plotted at 16:26:39 on 12/04/93 with Garfield version 4.06.

Fig.2. Cell in magnetic field (B=1 Tesla)

$\times 10^{-3}$ x(t)-Correlation plot
Gas ID = Argon 50% Ethane 50% Angle to y = 0.00 degrees
Wire no = 72 (type S)

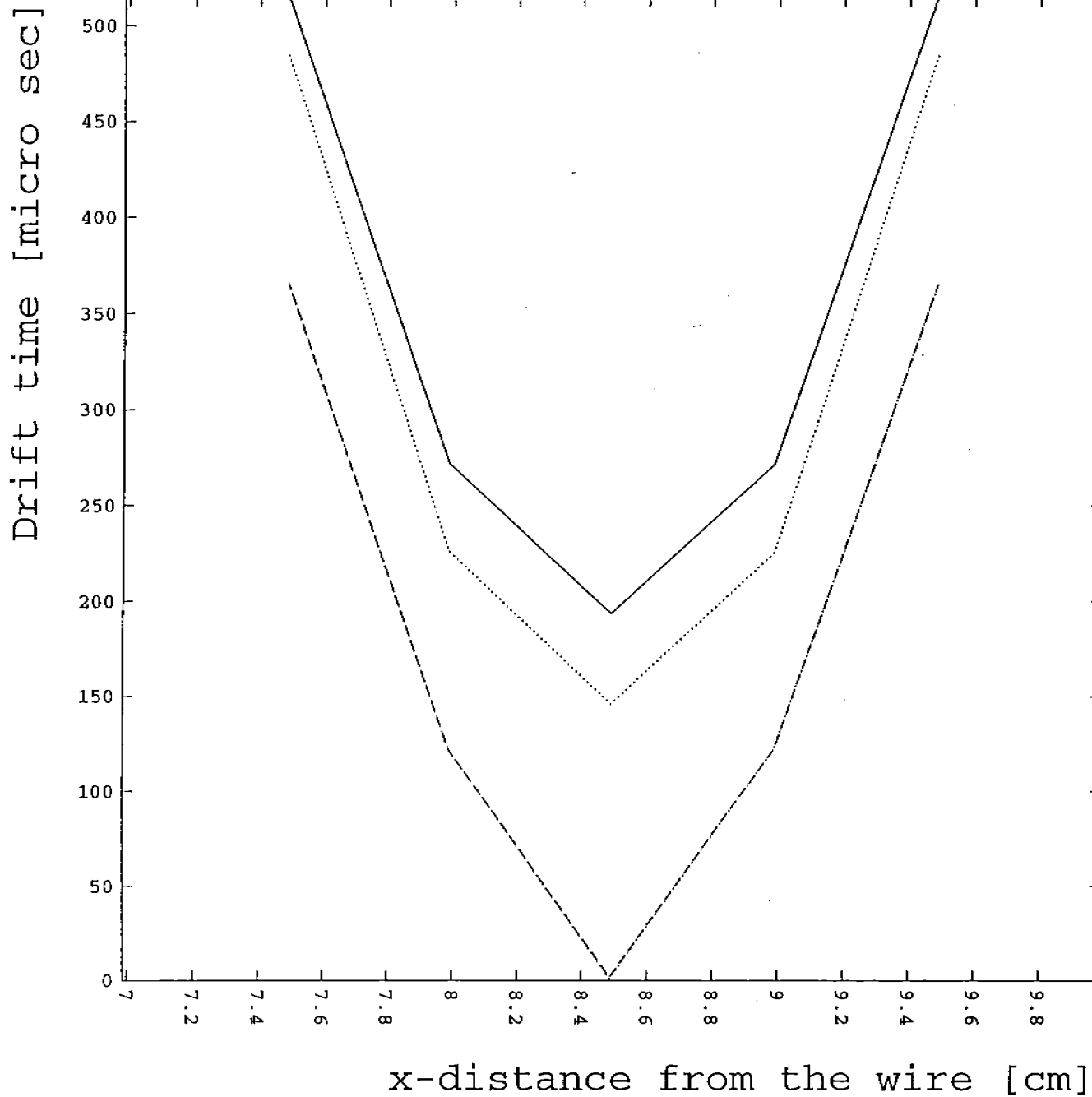


Plotted at 12:02:05 on 8/04/93 with Garfield version 4.06.

Fig.3. XT-PI OT output (R=0)

ARRIVAL TIME DISTRIBUTION

$\times 10^{-3}$
Gas ID = Argon 50% Ethane 50% Angle to y = 0.00 degrees
Wire no = 55 (type S)



Plotted at 16:36:28 on 12/04/93 with Garfield version 4.06.

Fig.4. ARRIVAL output (B=1 Tesla)

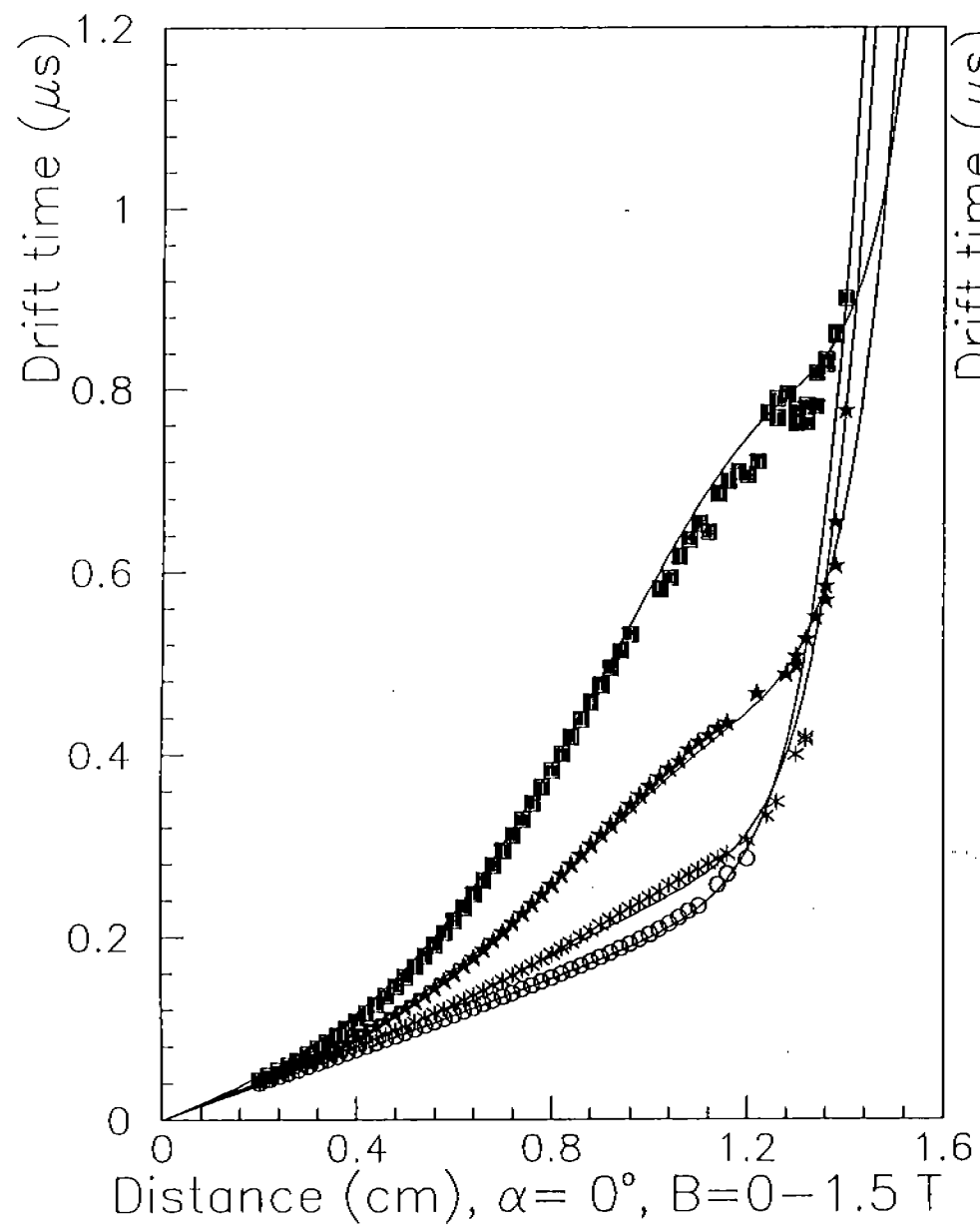


Fig.5a

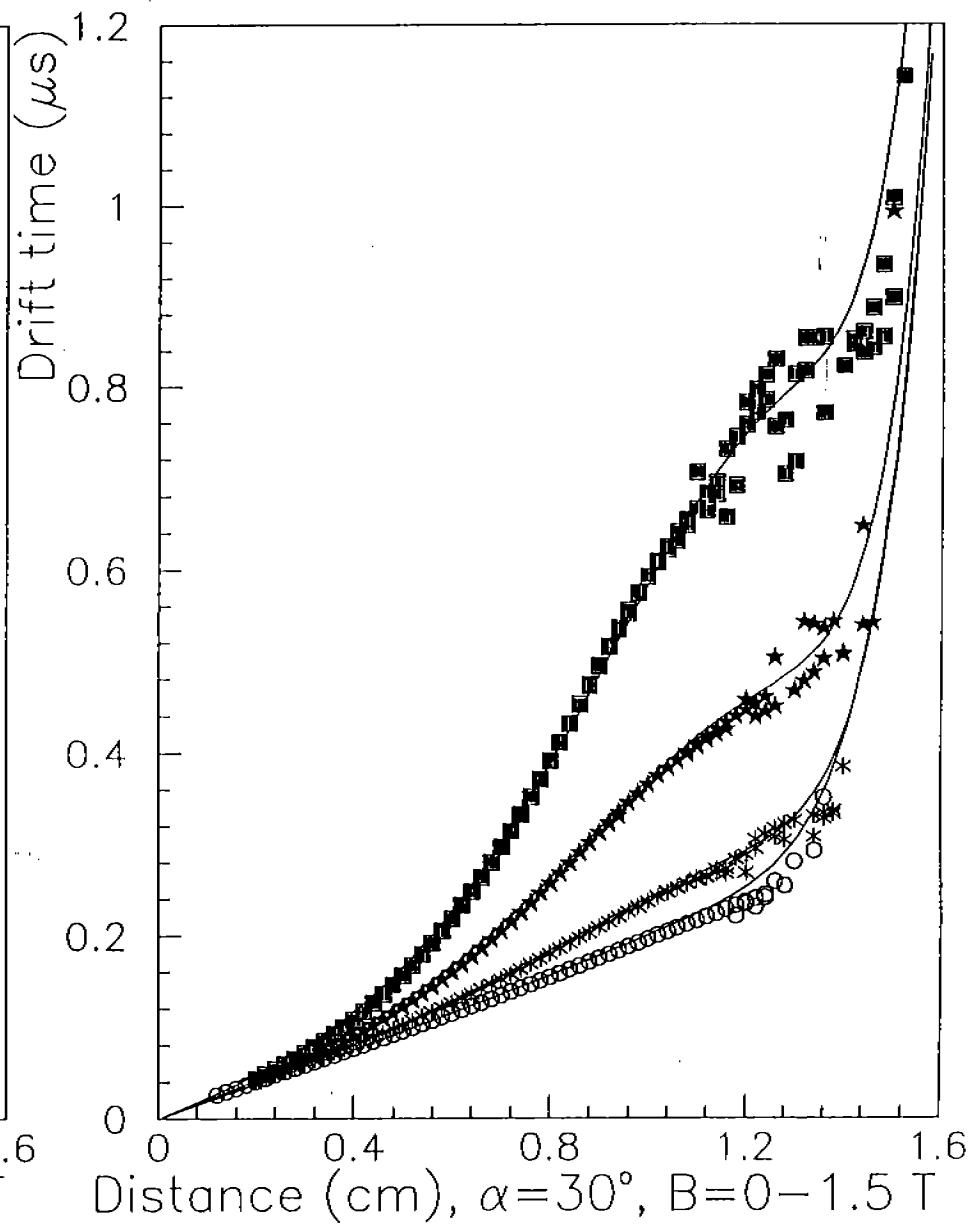


Fig.5b

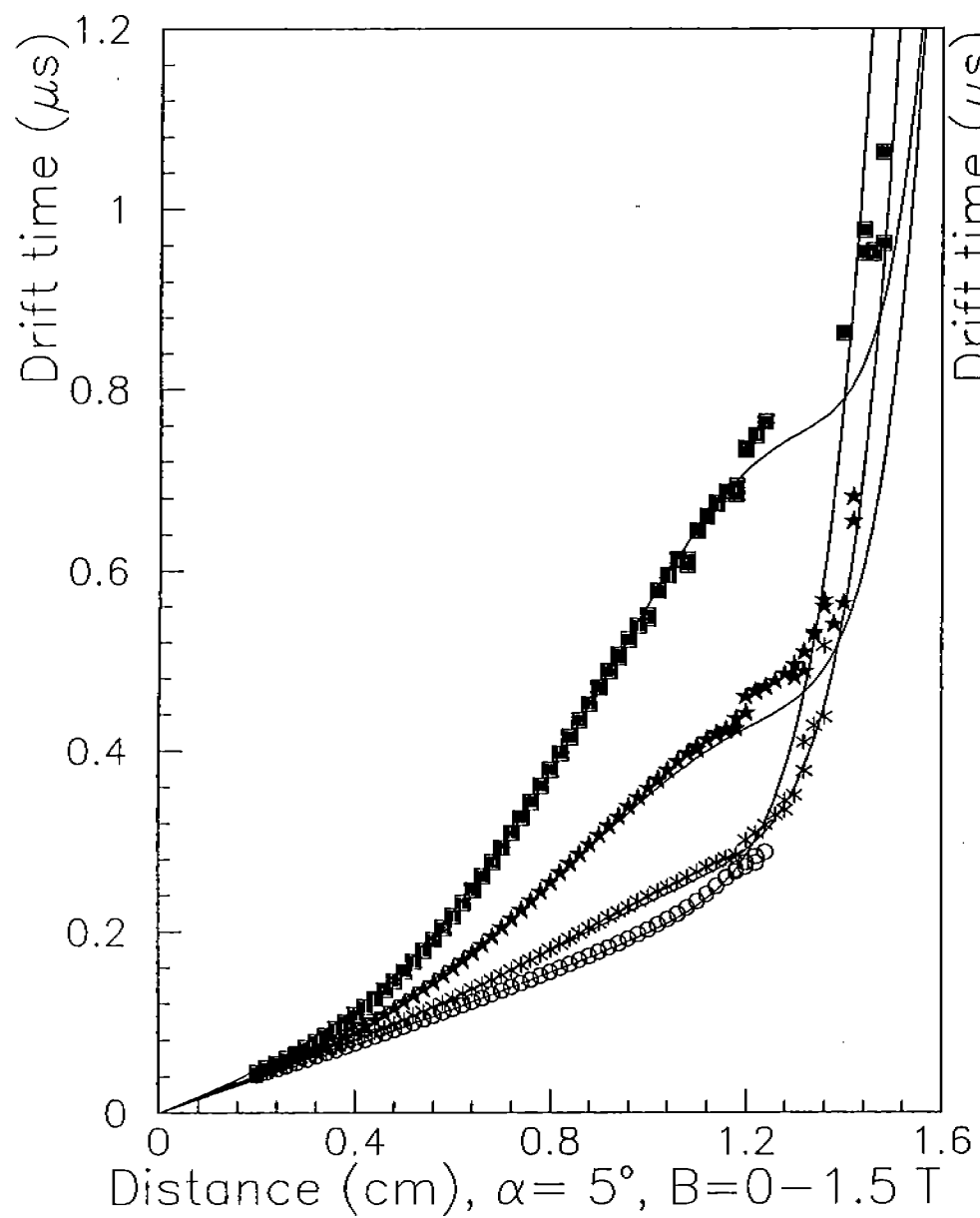


Fig.5c

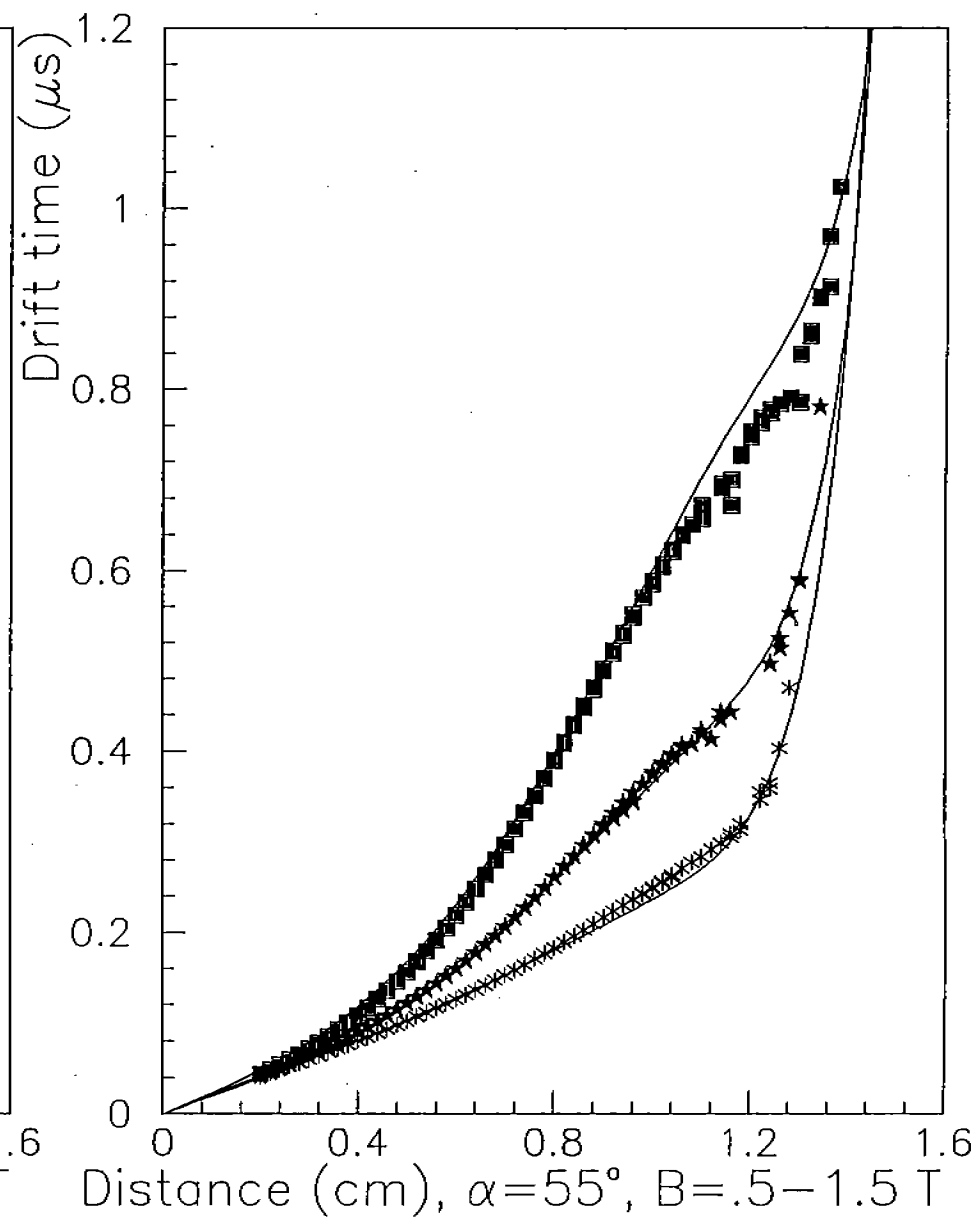


Fig.5d

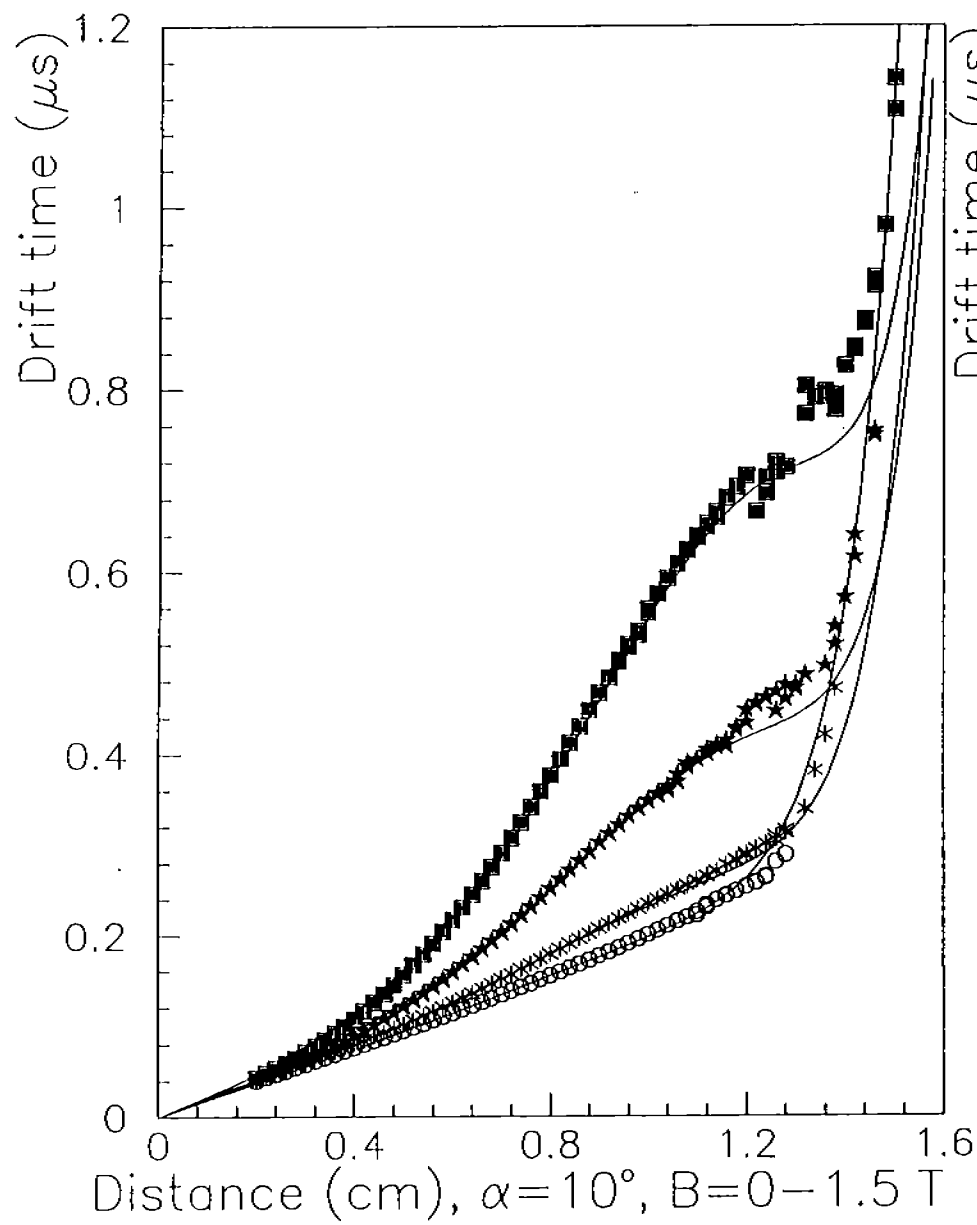


Fig.5e

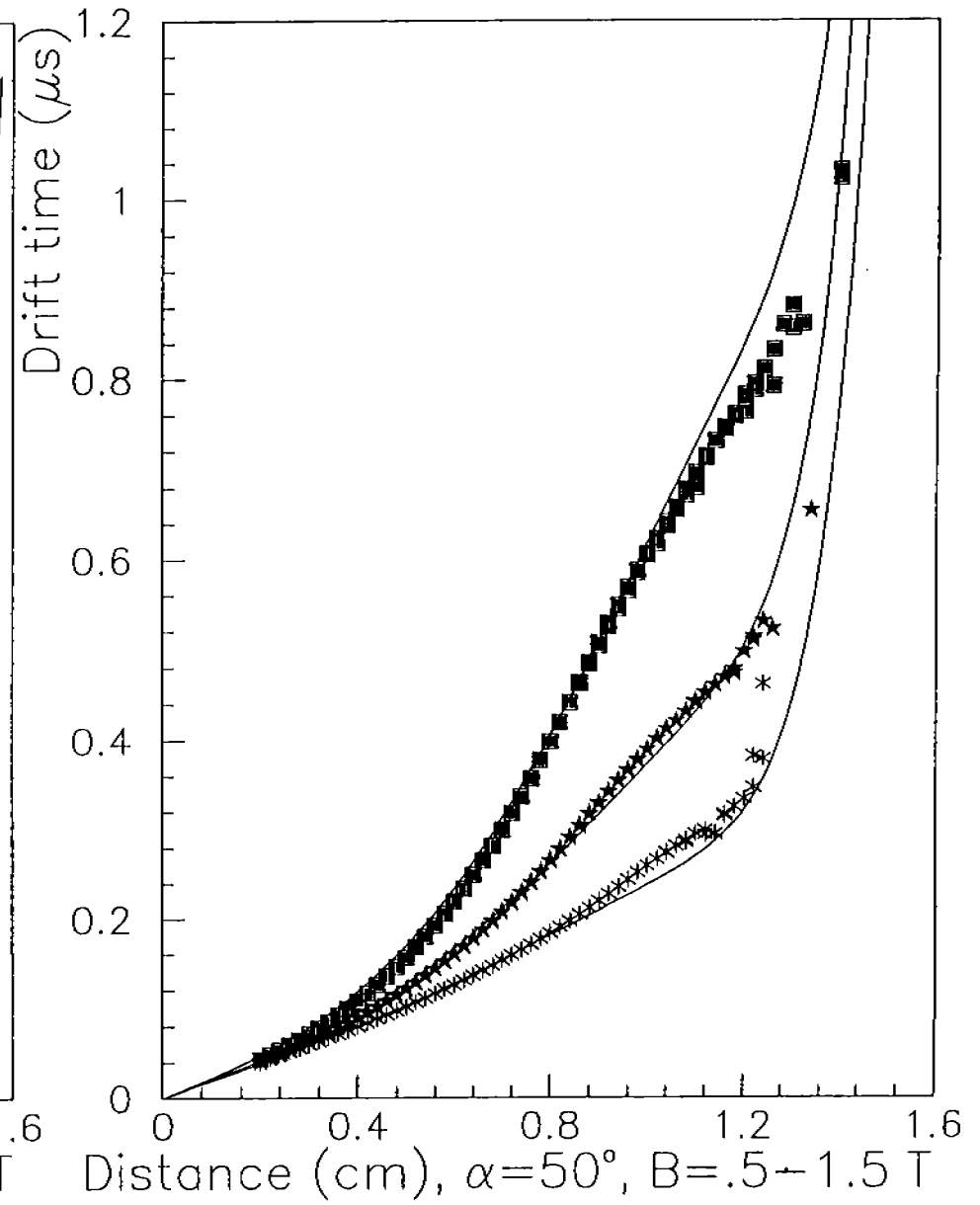


Fig.5f

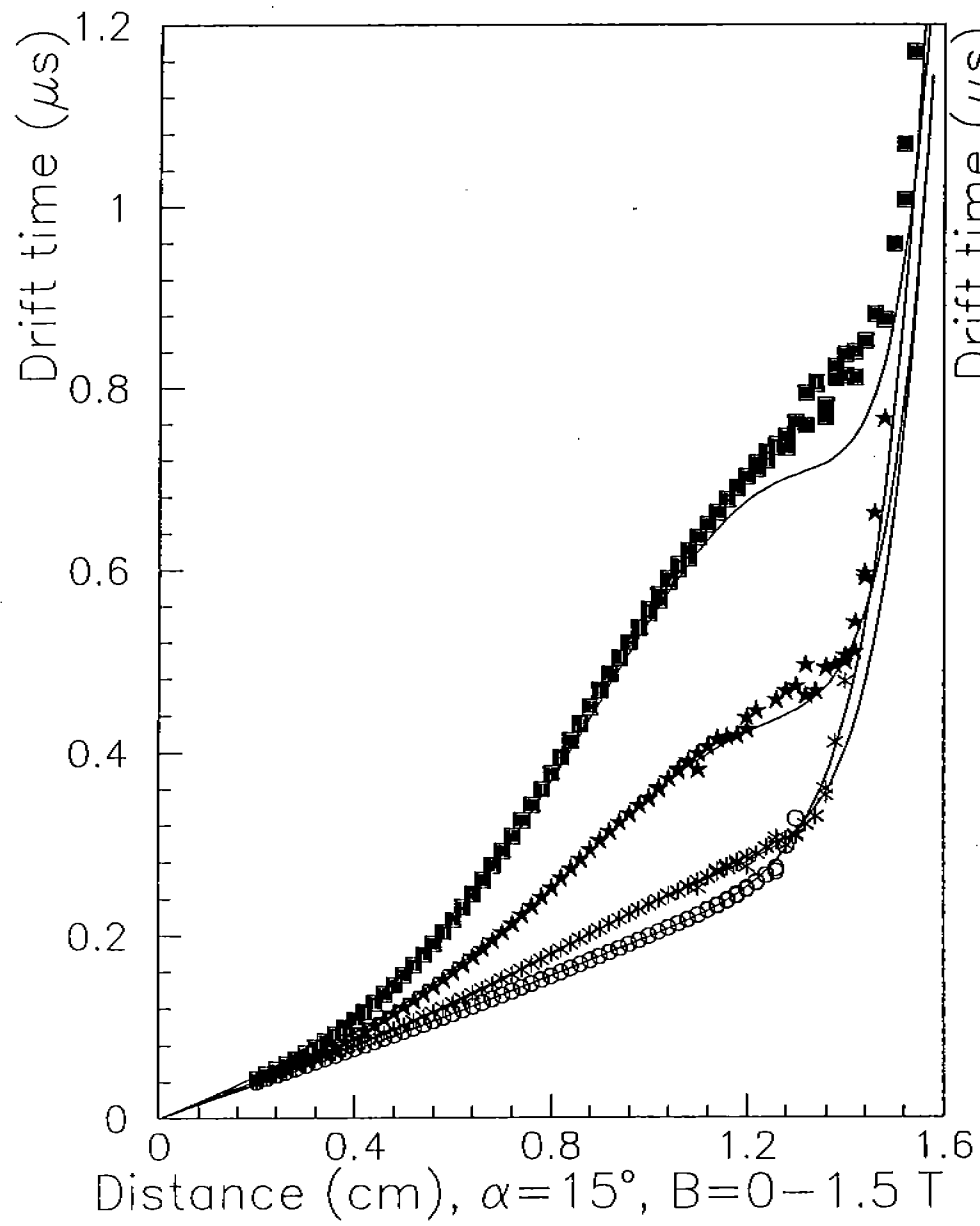


Fig.5g

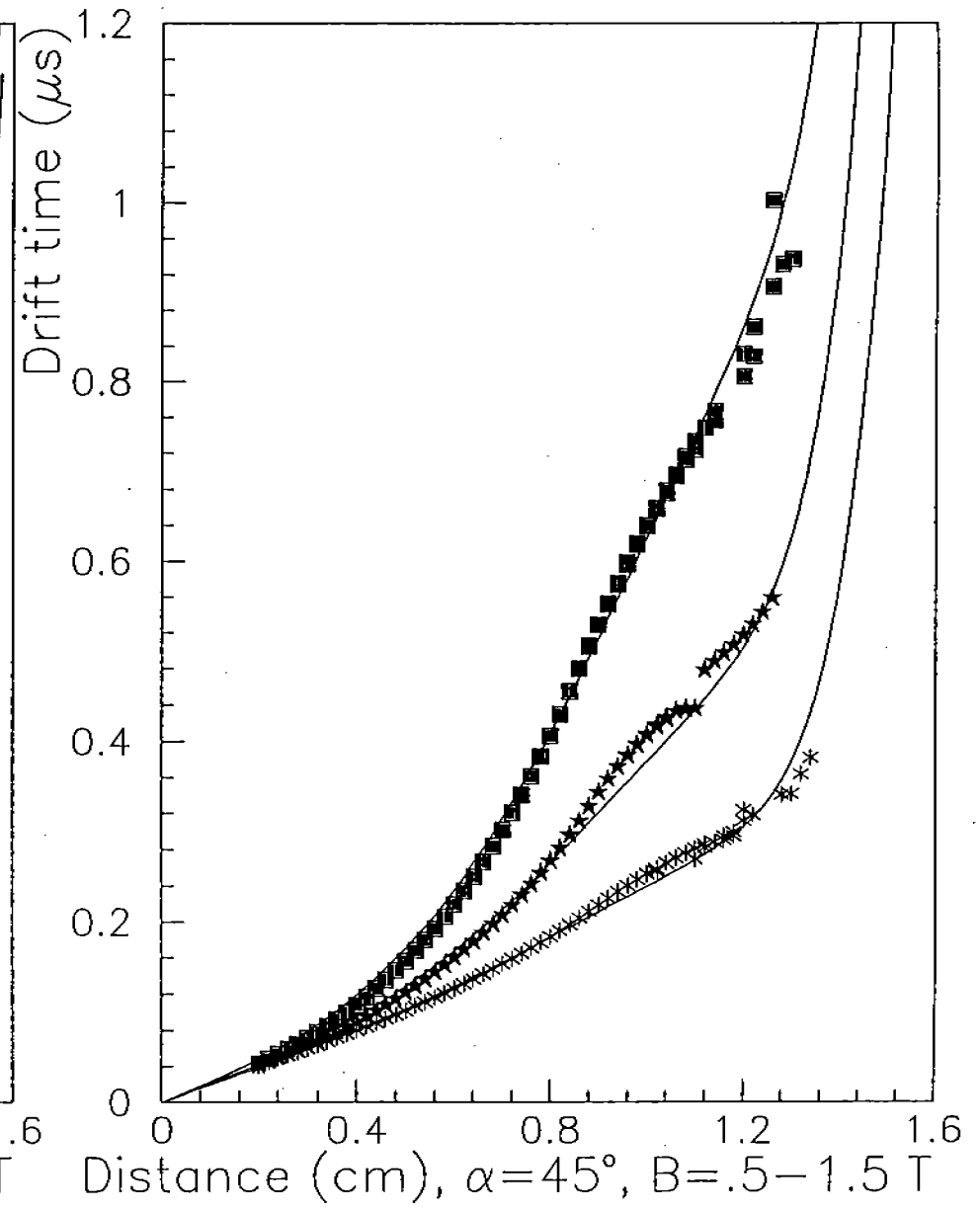


Fig.5h

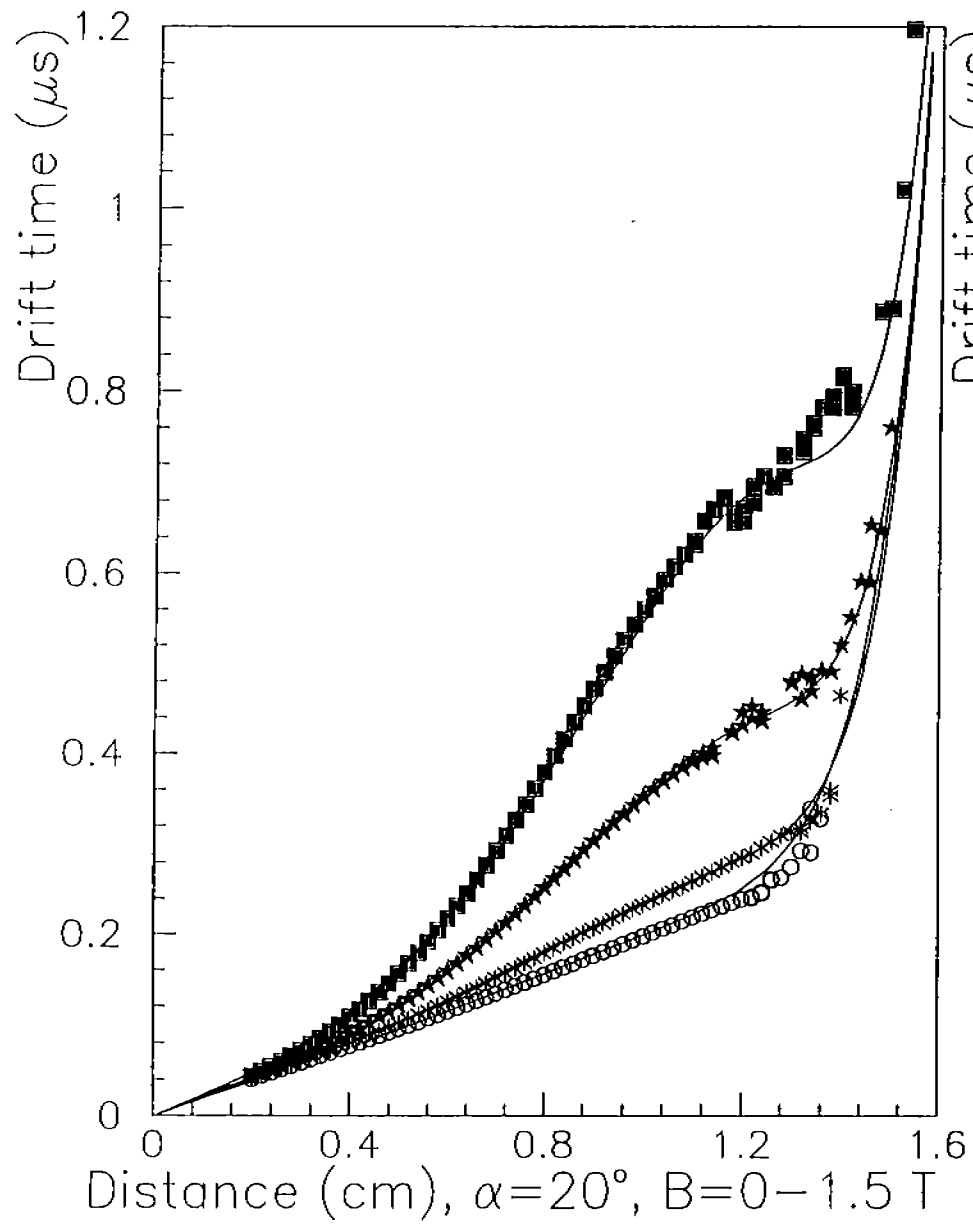


Fig.5i

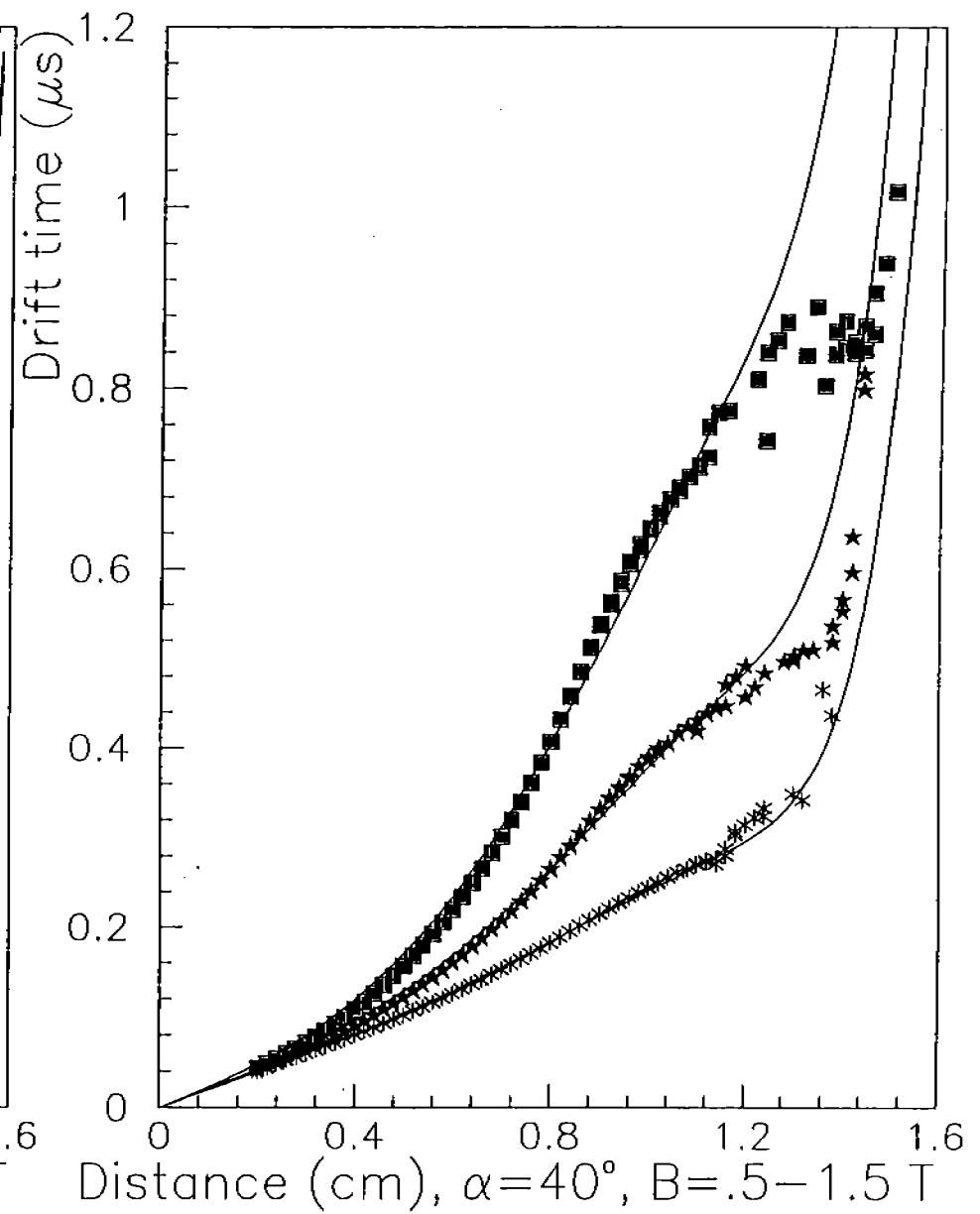


Fig.5j

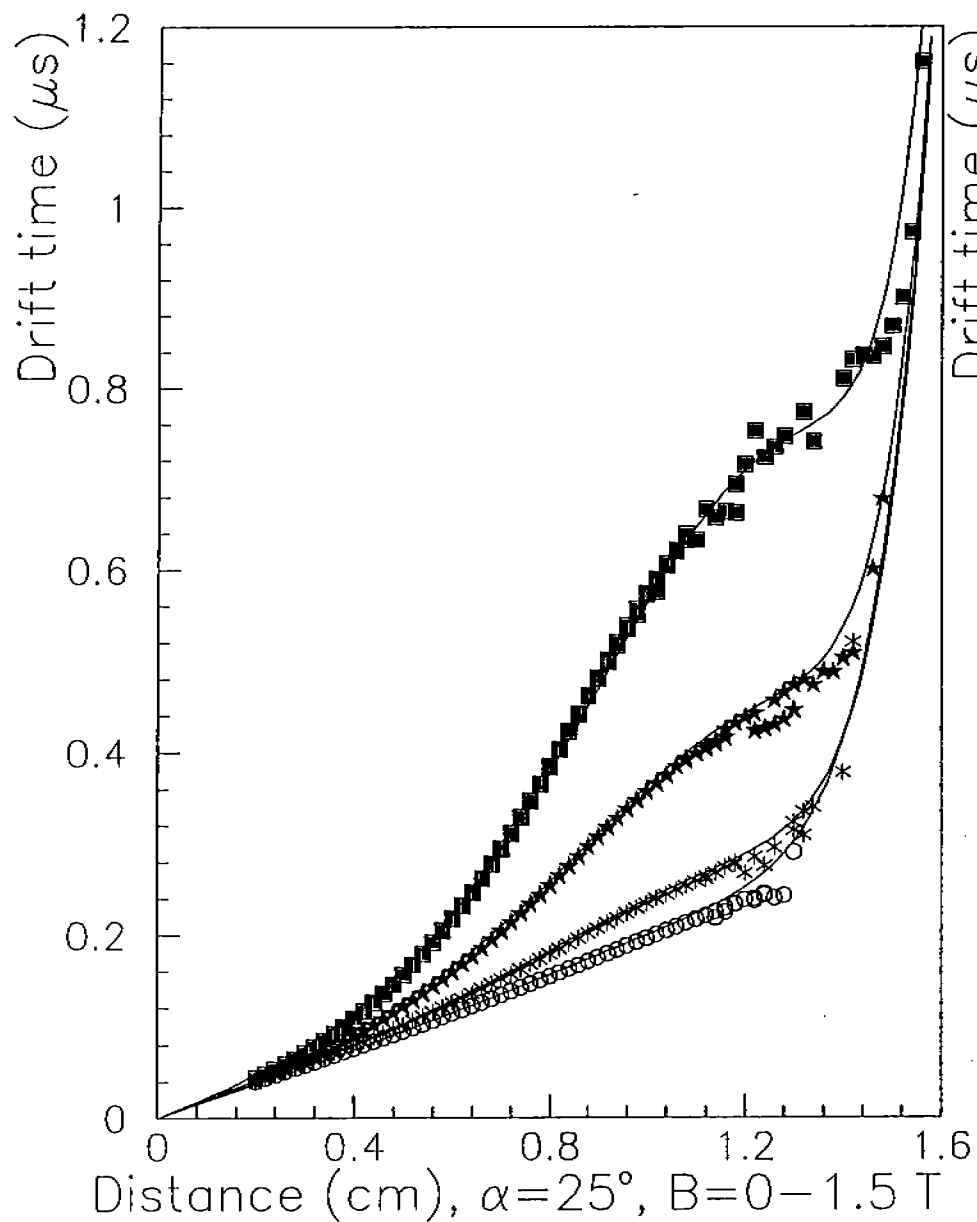


Fig.5k

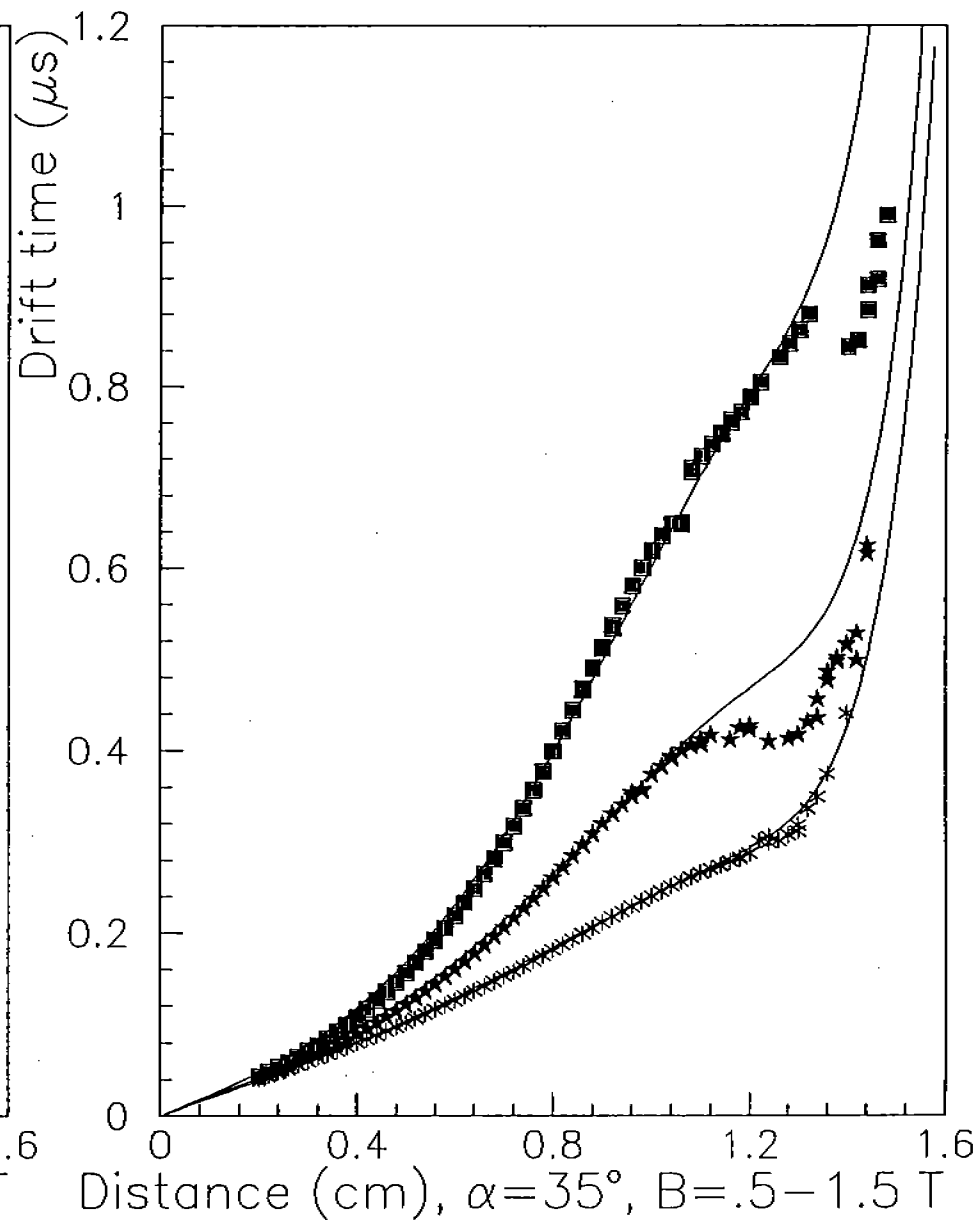


Fig.5l

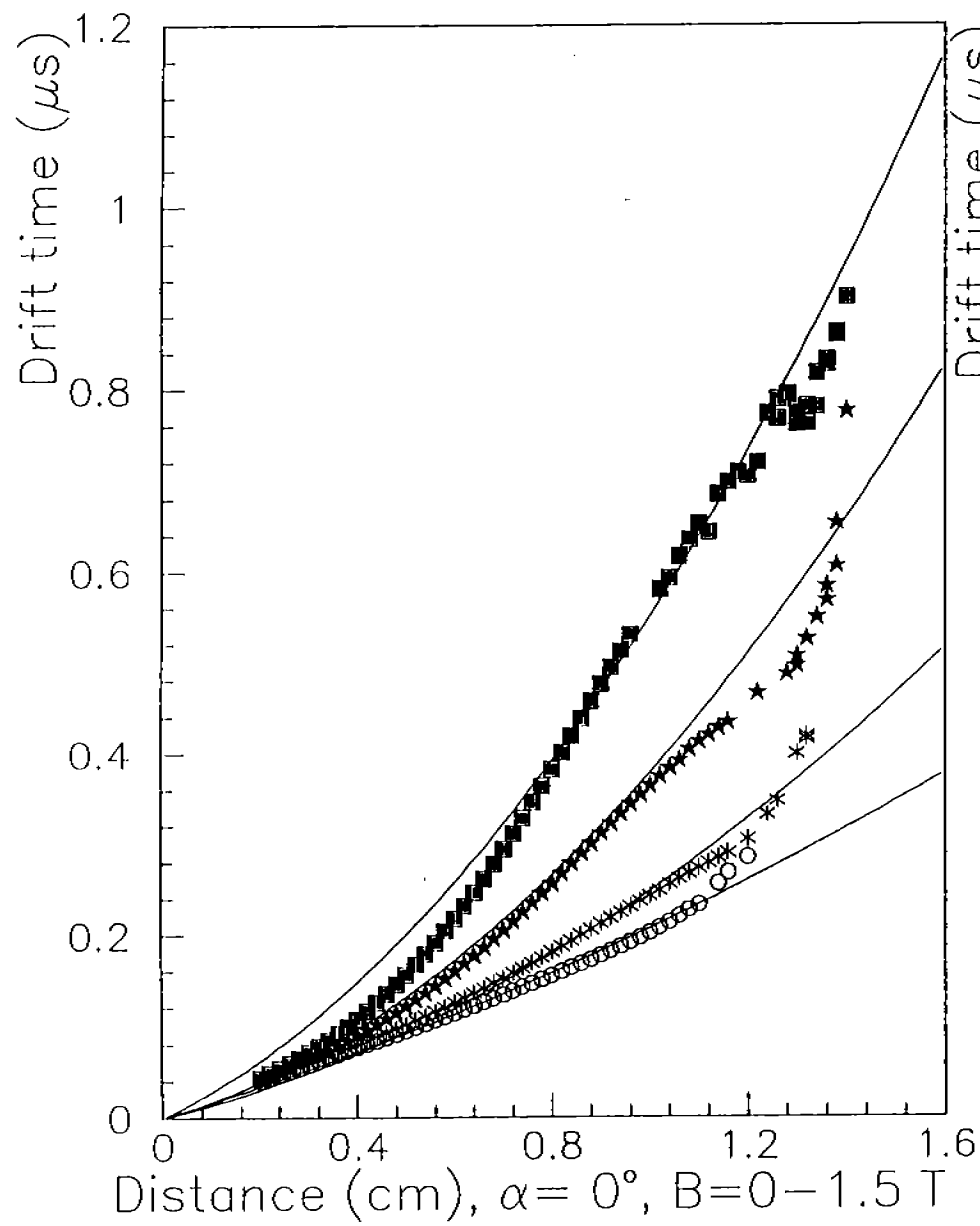


Fig.6a

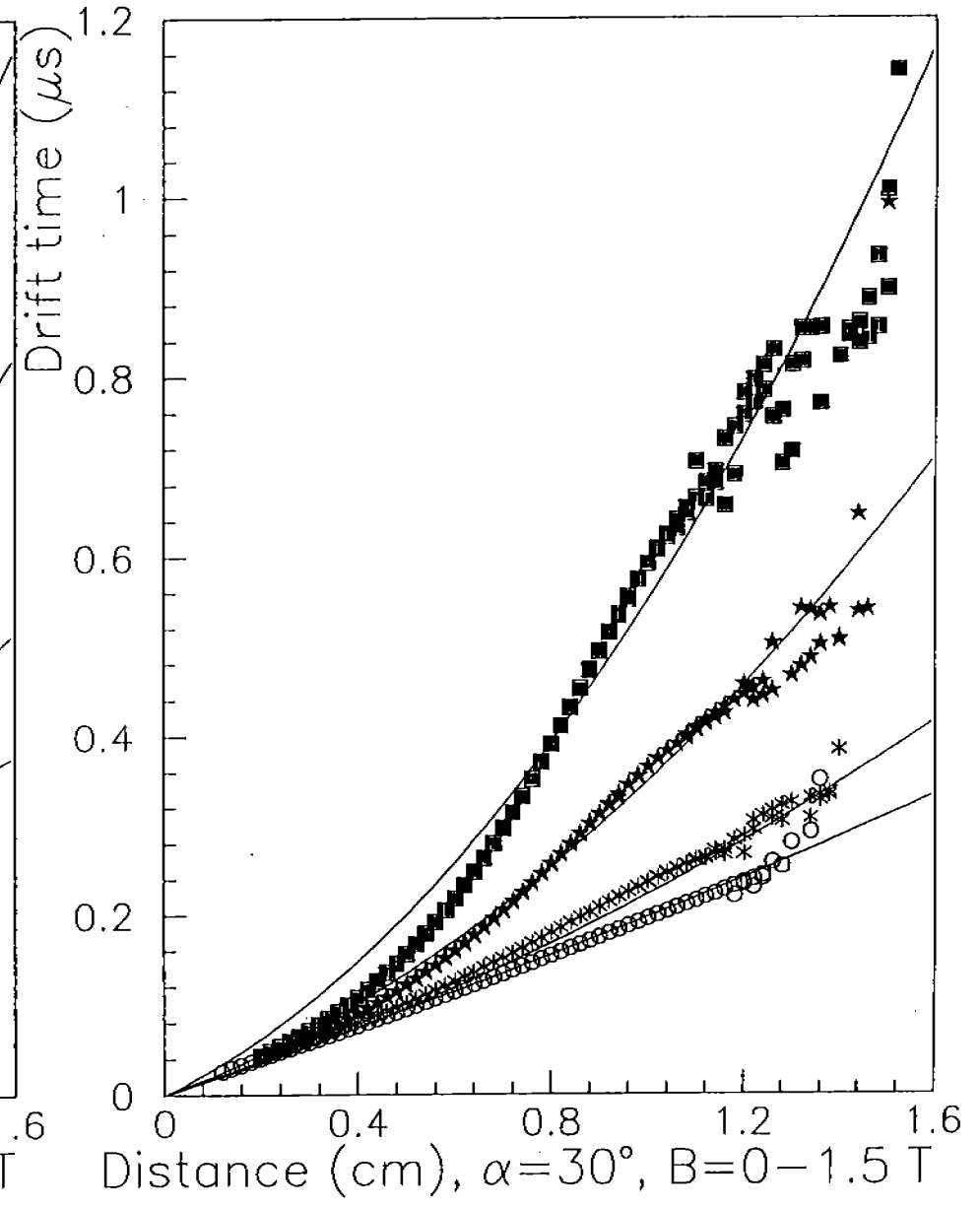


Fig.6b

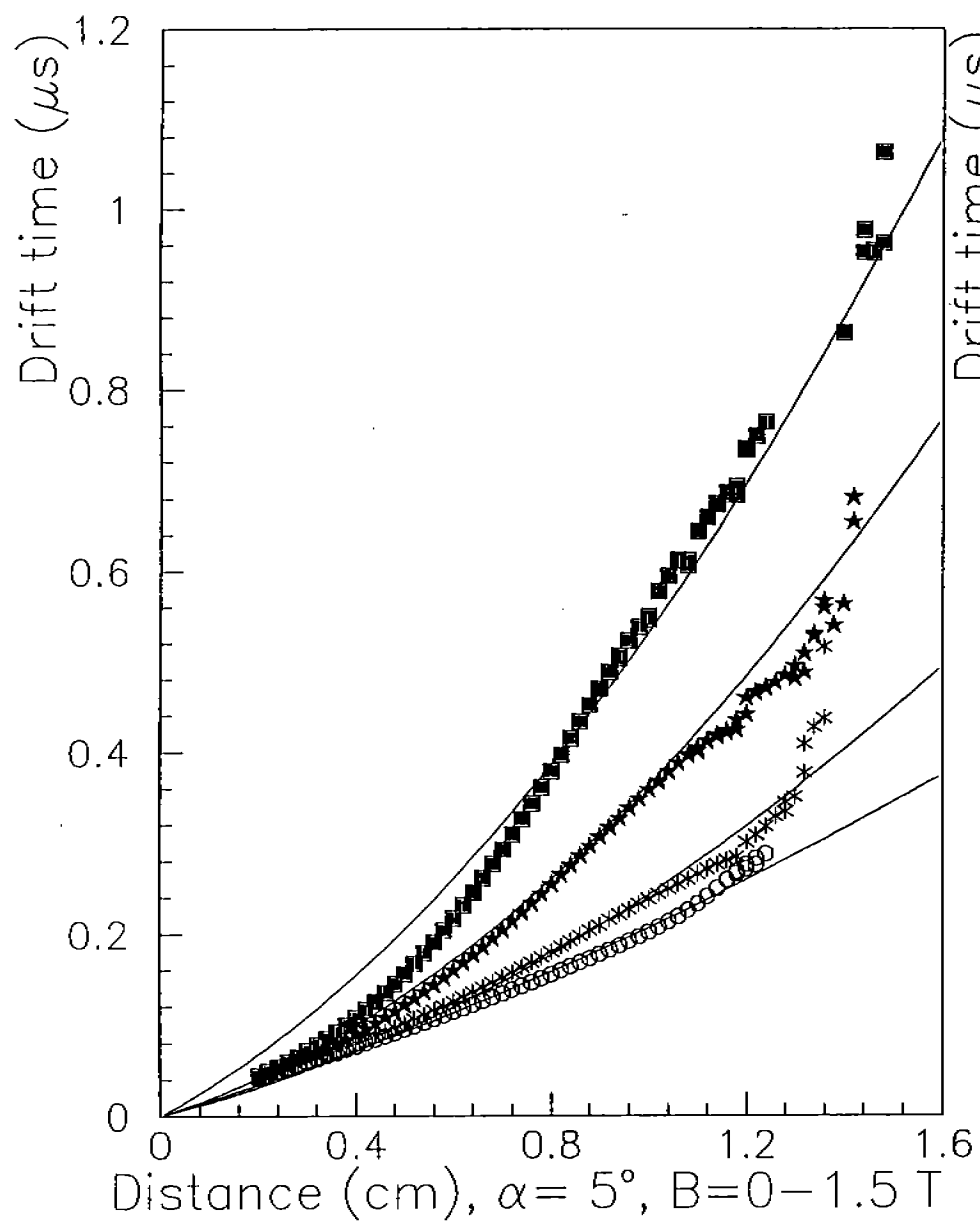


Fig.6c

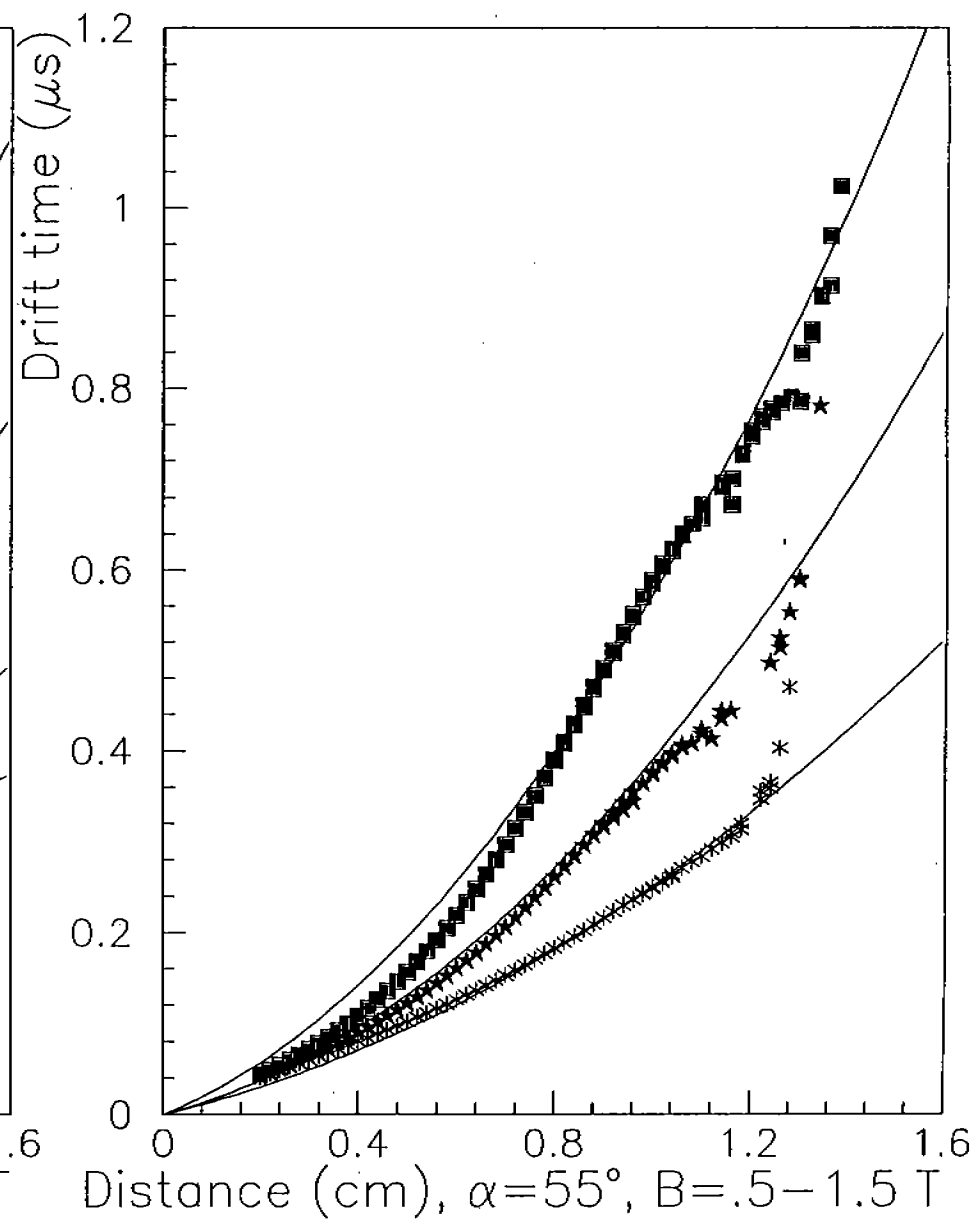


Fig.6d

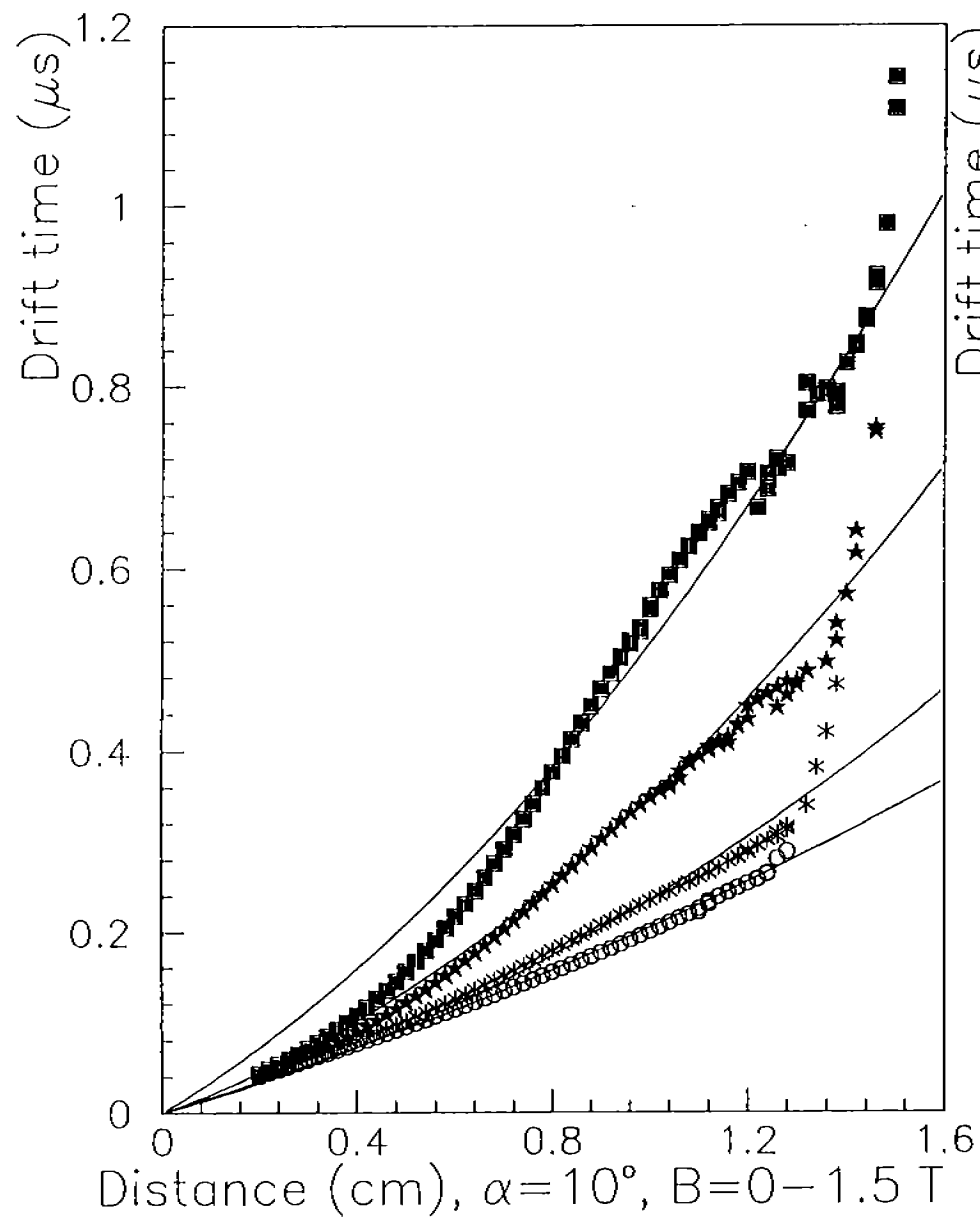


Fig.6e

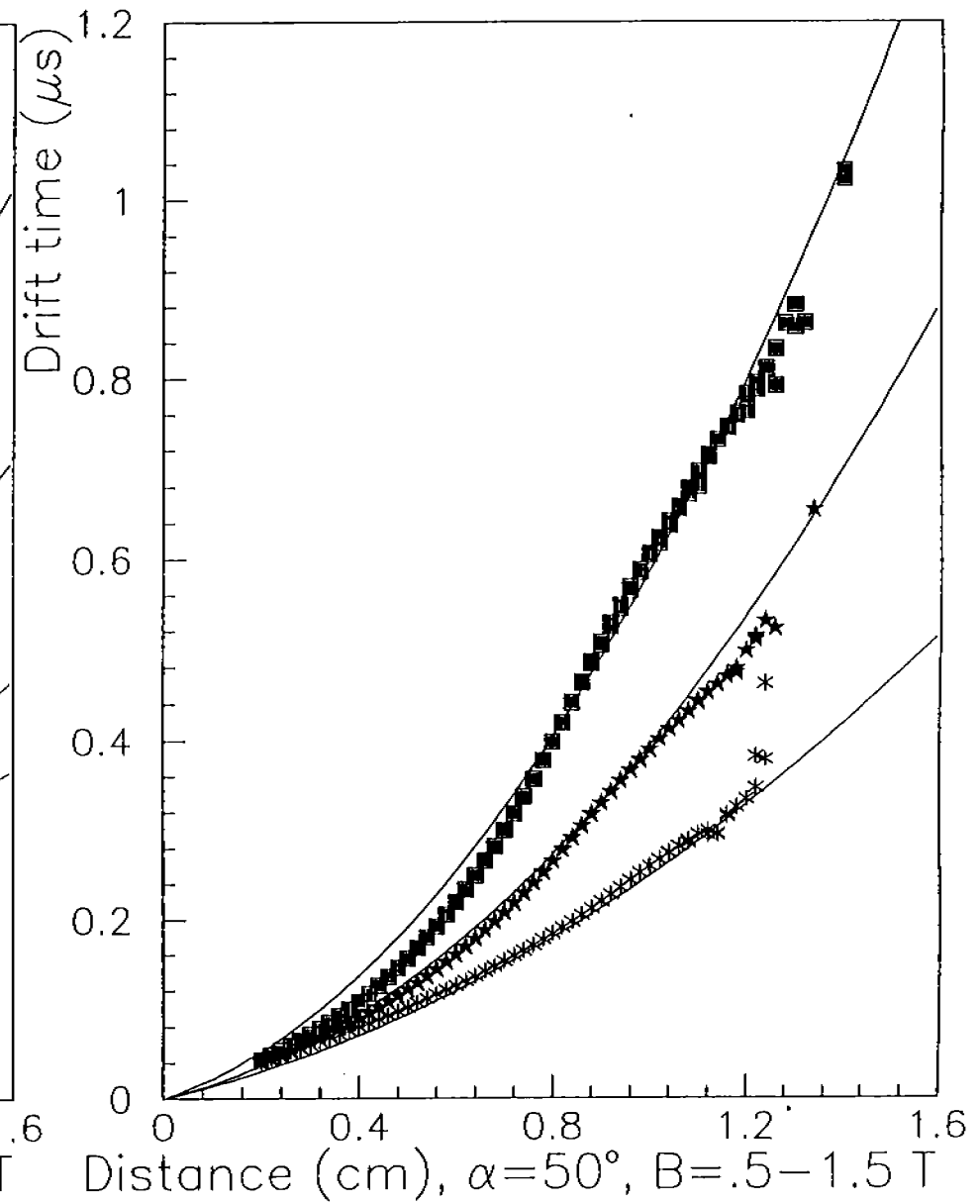


Fig.6f

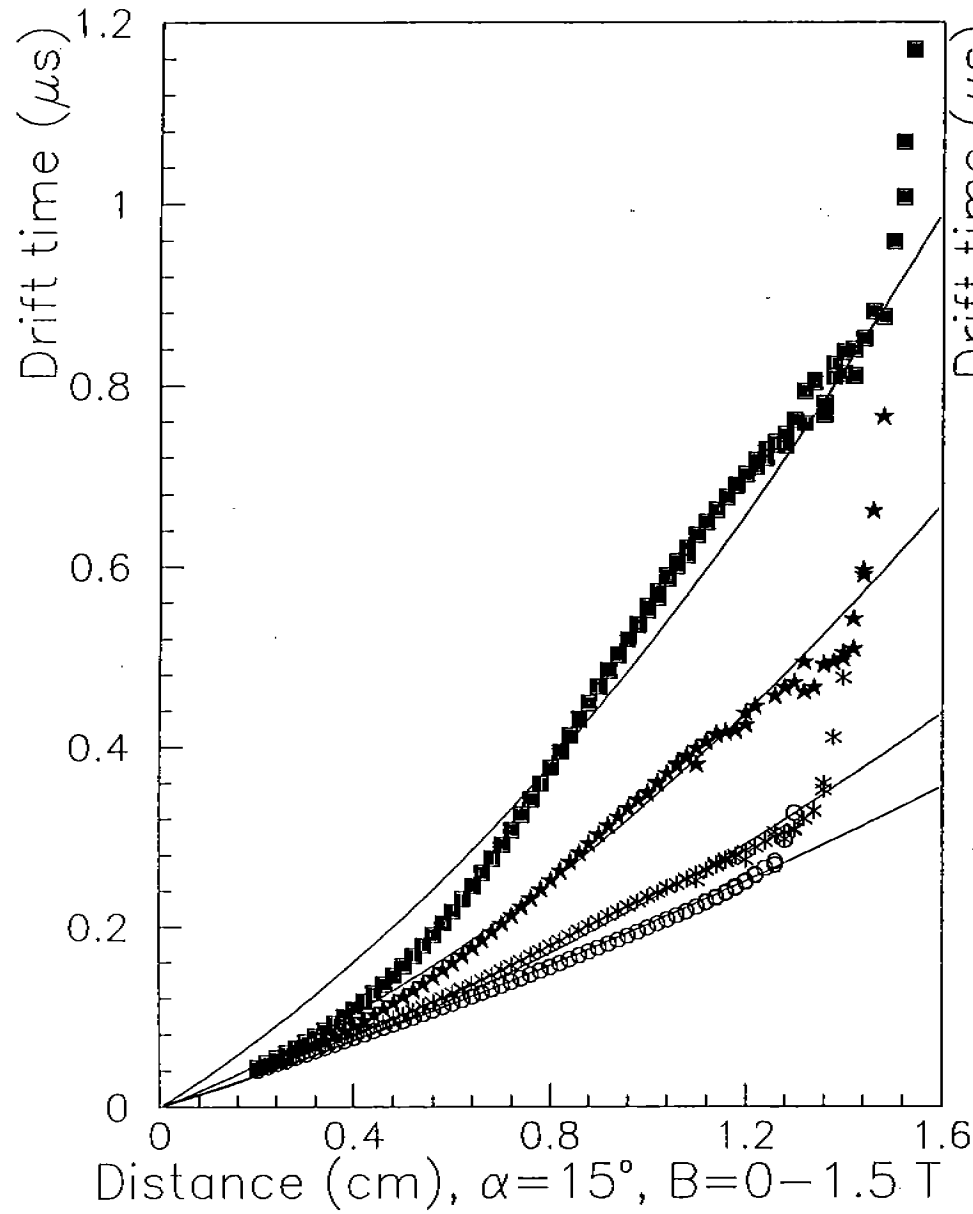


Fig.6g

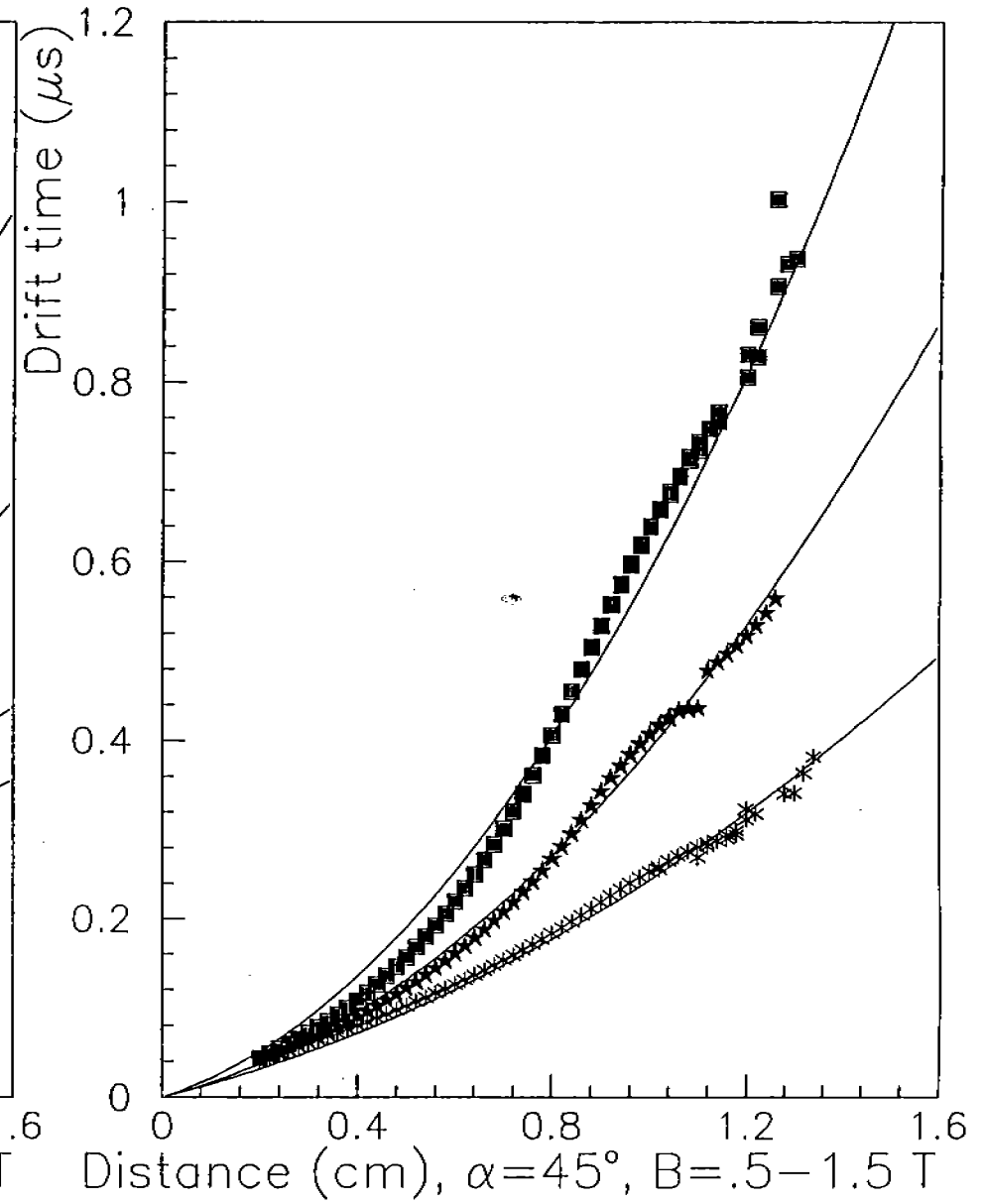


Fig.6h

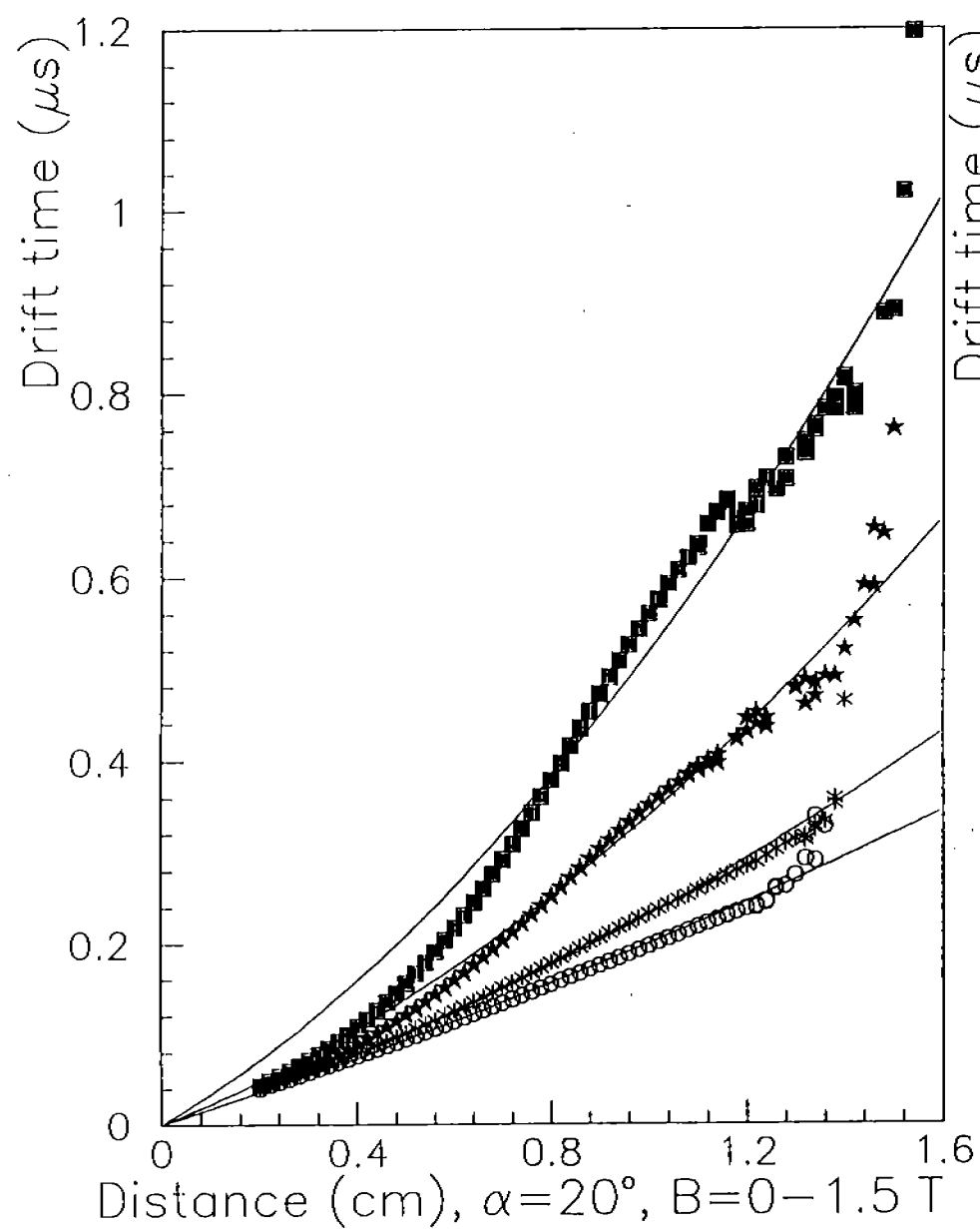


Fig.6i

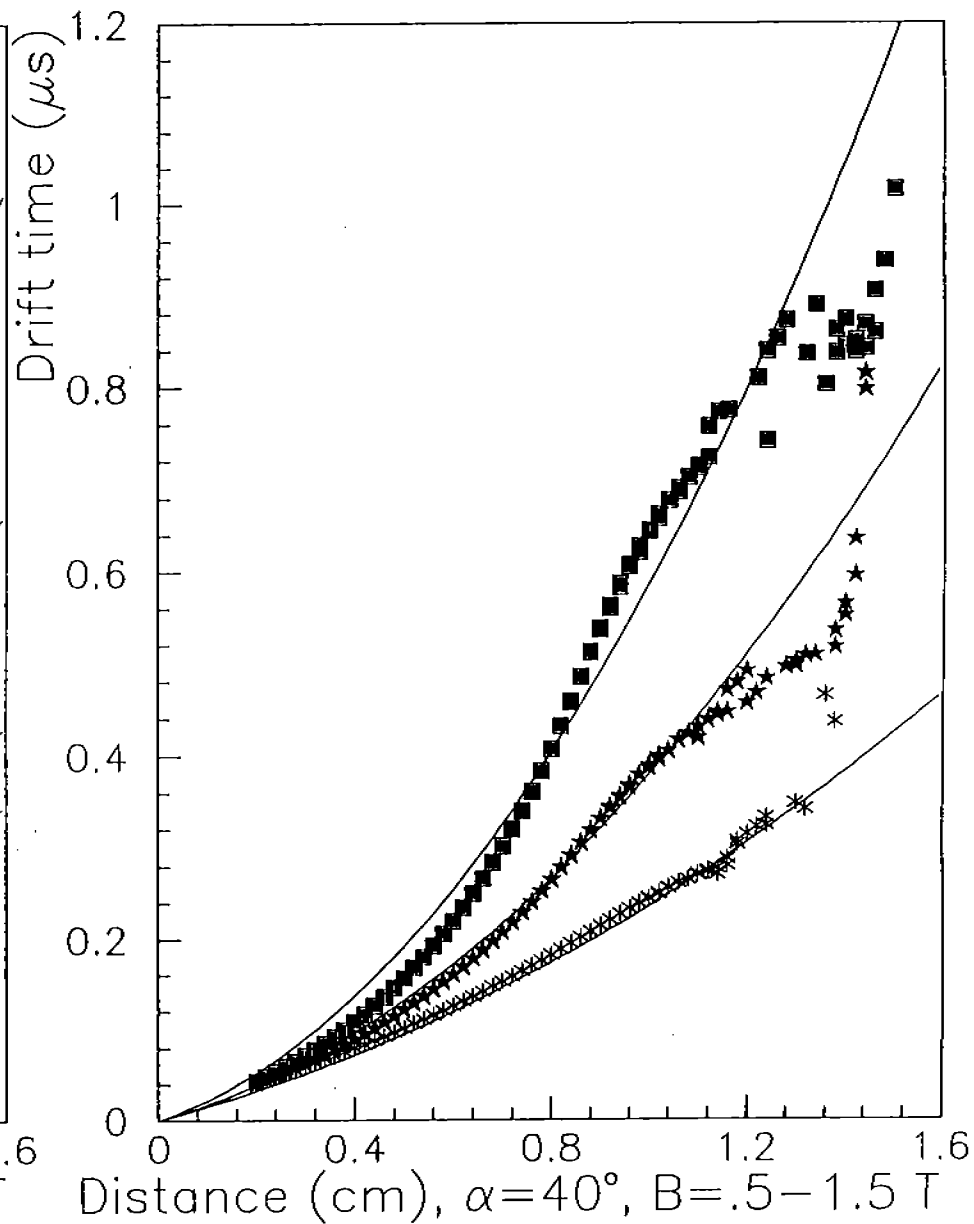


Fig.6j

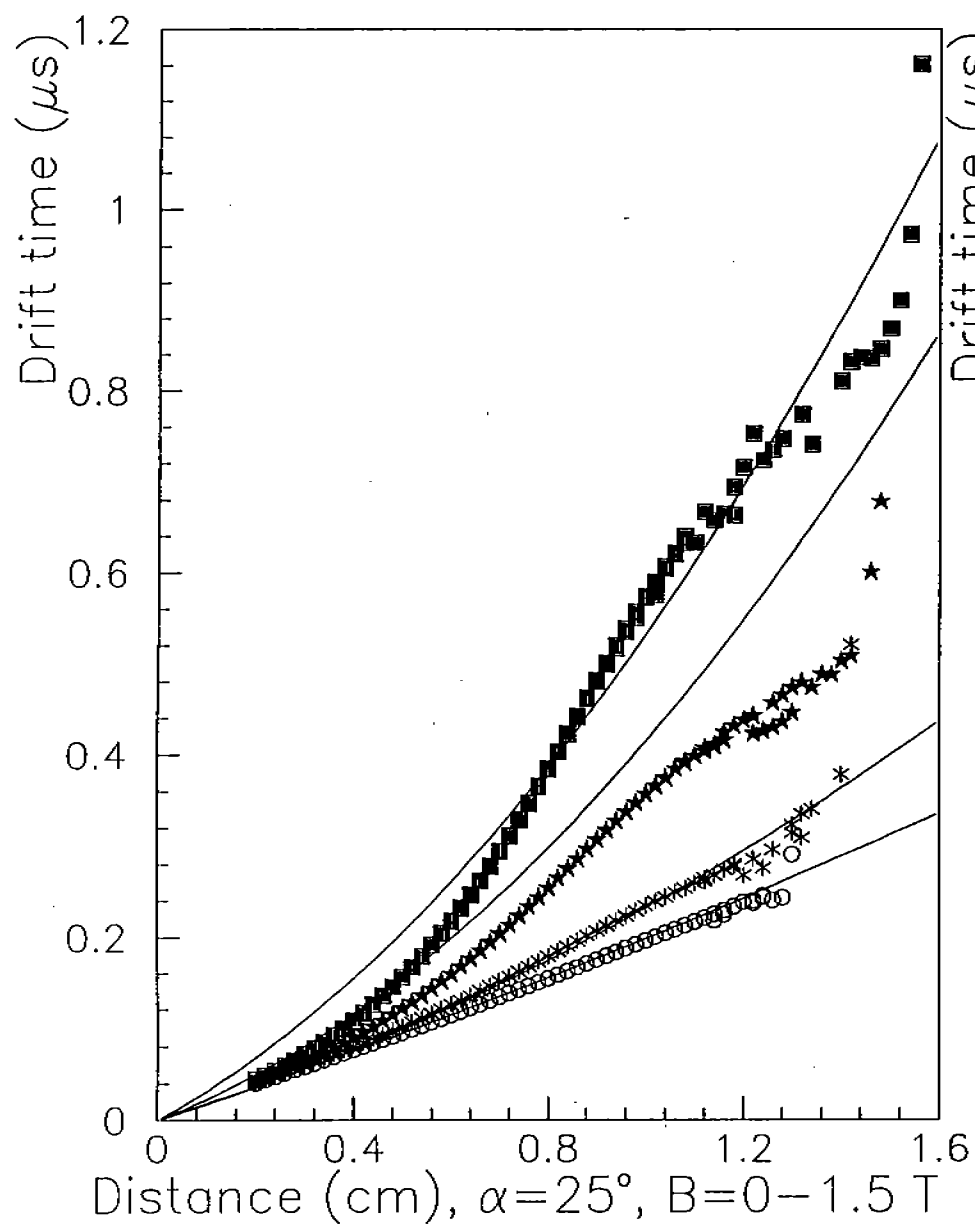


Fig.6k

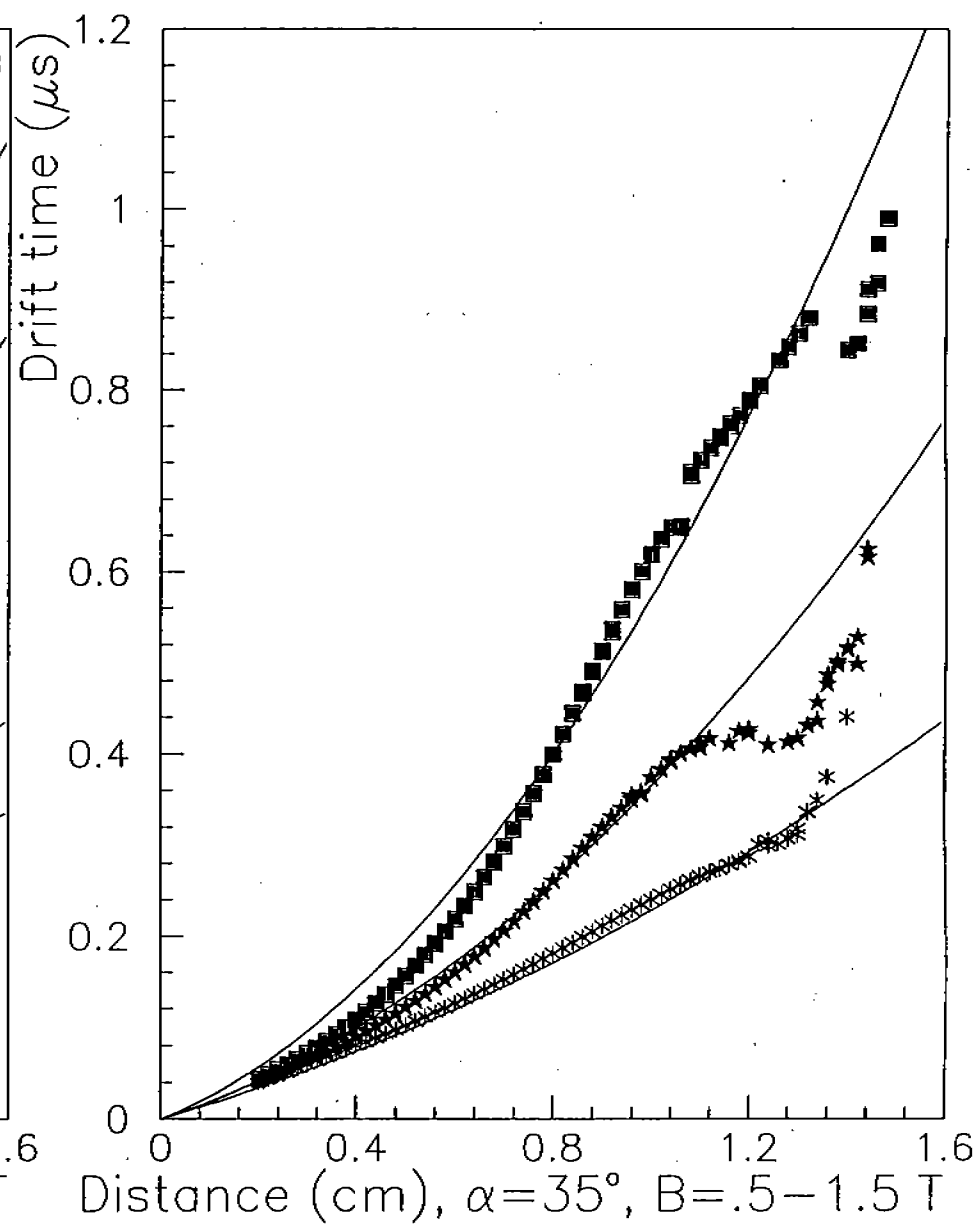


Fig.6l